N70-33995

JPL-760-

JPL-760-51

VEHICLE MOBILITY TESTS
SOFT SOIL SLOPES

June 25, 1970

N70-33995

JET PROPULSION LABORATORY
CALIFORNIA INSTITUTE OF TECHNOLOGY
PASADENA, CALIFORNIA

FOREWORD

The investigation documented in this report constitutes part of the Lunar Roving Vehicle (LRV) research conducted by the Advanced Lunar Studies (ALS) Team at the Jet Propulsion Laboratory*. These vehicle mobility tests have been performed to develop and provide a better understanding of mobility concepts on sloping terrains as applied to LRV.

*This work was performed by the California Institute of Technology for the National Aeronautics and Space Administration.

ACKNOWLEDGMENT

Contributors to this report include:

V. Anthony

M. Baligh

J. K. Hawkes

R. E. Imus

T. D. Lu

H. C. Primus

CONTENTS

CONTENTS (contd)

FIGURES

CONTENTS (contd)

FIGURES (contd)

I. SUMMARY

Experimental results of a short series of exploratory tests are presented which investigate the character of the soft soil slope climbing problem. These experiments include:

(1) Laboratory tests of loaded plates on sloped sandy soils:
These tests investigate the interaction of normal and shear forces on sloped sandy surfaces using simple loaded plates. The limited results indicate the general influence of slope, depth of penetration, and surface roughness on the ratio of maximum shear to normal stress in sandy soils.

(2) Vehicle slope climbing tests in soft soil:
These tests investigate slope climbing performance in the low wheel/soil pressure regime (0.2 to 0.7 lb/in.^{2}) using the six wheeled Surveyor Rover (SLRV). The general results indicate the inadequacy of current horizontal wheel tests to determine vehicle slope climbing performance and point out the dependence of drawbar pull versus slip curves on the soil slope.

These tests suggest the following areas for further exploration in developing analytical slope climbing methodology for design:

(1) Rigid and flexible wheel slope climbing tests.

(2) Extended simple plate tests on sandy slopes to help interpret the results of wheel slope climbing tests.

(3) Wheel/soil interface friction tests (with different materials).

II. INTRODUCTION

An effective lunar and planetary program for roving vehicles requires some advanced information about the behavior characteristics (soil support and thrust for vehicle mobility) of the various terrains that may be encountered. Current testing concepts of vehicle mobility generally refer to horizontal terrains. Information about soft, steep-sloped surfaces for estimating vehicle performance is limited because of the more complex problems involved.

At JPL, a minimum exploratory testing program has been conducted for investigating vehicle mobility performance on soft, level and sloping terrains. Specific information is given about vehicle characteristics, soil material, equipment, and instrumentation along with an analysis of the test results.

The basic objectives of these tests were to: (1) obtain vehicle performance data on soft, steep slopes for potential lunar applications assuming low soil-wheel contact pressure of less than 0.75 lb/in.^{2} and small sinkages, (2) establish criteria for planning more representative single wheel tests on slopes, and (3) guide the formulation of a mathematical soil-wheel interaction model for horizontal and sloping terrains.

It is not the purpose of these tests to derive specific values for the design of Lunar Roving Vehicles, but mainly to clarify the mechanics of soft-soil slope climbing and point out some salient aspects of this process. It is recognized that the testing data are limited due to the exploratory nature of this program, but the trends and general conclusions arrived at are significant in providing a basic understanding of this research subject. A major motivation in planning these tests was the lack of fundamental information of slope climbing and soil-wheel interaction on level terrains with very low pressure. This constitutes an area of vehicle operation having significant potential implication for lunar vehicle mobility missions.

The soils considered were an air-dried, cohesionless sand and a wet sand with mixed frictional and cohesive properties. Slopes were prepared artificially and varied up to near the angle of repose.

III. MOBILITY ON STEEP SLOPES

Immobilization in climbing soft soil slopes is due to either one or the combination of the following factors: (1) lack of soil-wheel interface friction which would enable the soil to transfer the thrust for mobility purposes, and (2) exceeding the slope bearing capacity for the combined loads of vehicle weight and thrust required for mobility. In both cases, with an increasing slope, wheel rotation produces a down-the-slope soil transport accompanied by larger wheel sinkages under continuously degrading conditions. A LRV with limited maneuvering capability may be unable to extricate itself from the inside of a crater if either of the above limiting conditions is reached.

In principle, the study of soil-wheel interaction points to two basic aspects. One corresponds to the operational conditions of a vehicle whereby mobility is always guaranteed, particularly for low contact pressures and reduced sinkage. In these cases, the design objective for mobility is mainly concerned with an optimization problem. The other aspect relates to the limiting operational conditions of a vehicle on steep slopes where the slope reaches its limiting equilibrium state due to soil weight. In this case, mission safety rather than efficiency constitutes the constraint factor.

Conceptually, the problem of soft soil-wheel interaction covers the normal vehicle operation up to and including immobilization. Each case is intimately connected with a specific soil failure condition. Thus, the problem of soil-wheel interaction pertains to the study of soil mechanics and the theory of plasticity.

Table 1 indicates the implemented test program in which the various conditions of soil-wheel interaction were explored.

TABLE 1. SLRV MOBILITY SLOPE TESTS

Vehicle weight, lb	Slope, deg				
	Dry sand		Wet sand		
158	0	20		30	35
40	-	-	25	-	35

IV. TEST FACILITY AND OPERATION

Figure 1 is a sketch showing the sloped soil testing facility. Figure 2 shows an overall view of the facility, with the test vehicle, before sand had been laid on the horizontal and sloped surfaces. A site was chosen which included a horizontal portion consisting of a concrete pavement which was adjacent to an existing slope upon which the inclined portion was erected.

Soil retaining walls spaced 6 ft 6 in. apart were constructed of plywood and erected as indicated; they contain the sand bed which was used for the horizontal and sloped soil track. The indicated dimensioning provided a soil track bed which permitted developing mobility across two vehicle lengths, or 12 ft, on both horizontal and sloped portions. Three-quarter inch pipe rails were supported on each side wall by lengths of two-by-fours whose position on the side walls could be changed to allow adjusting the soil slope from 20 to 40 degs as indicated in broken line in Fig. 1.

The pipe rails served as a means for guiding and supporting the soil hopper used for spreading sand to form the soil bed. The height above the plywood base for the bed and the angle at which the two-by-fours were mounted on the side walls determined the angle of the soil bed. Inclined portion of the pipe rails could be adjusted by pivoting the two-by-fours. The transition between the horizontal and inclined sections of the rail was made by a series of segmental blocks carrying small sections of pipe inserted between the two sections. This provided a smooth transition for connecting the two sections while maintaining the radius of curvature required for passage of the carriage frame. This frame also supported a counterweighting arrangement for lightening the load applied by the vehicle to the sand bed for tests involving less than full vehicle weight.

The soil bed, as shown in Fig. 3, was laid on the horizontal concrete section and on the sloped plywood bed by means of the hopper, shown in Fig. 4. The hopper was constructed of plywood, steel-reinforced, and was of 6 ft^3 capacity. It permitted pouring sand at a constant rate through a controlled opening across the full track width. The hopper was supported within the carriage frame on end pivots which allowed the hopper to swivel freely as the carriage was displaced back and forth.

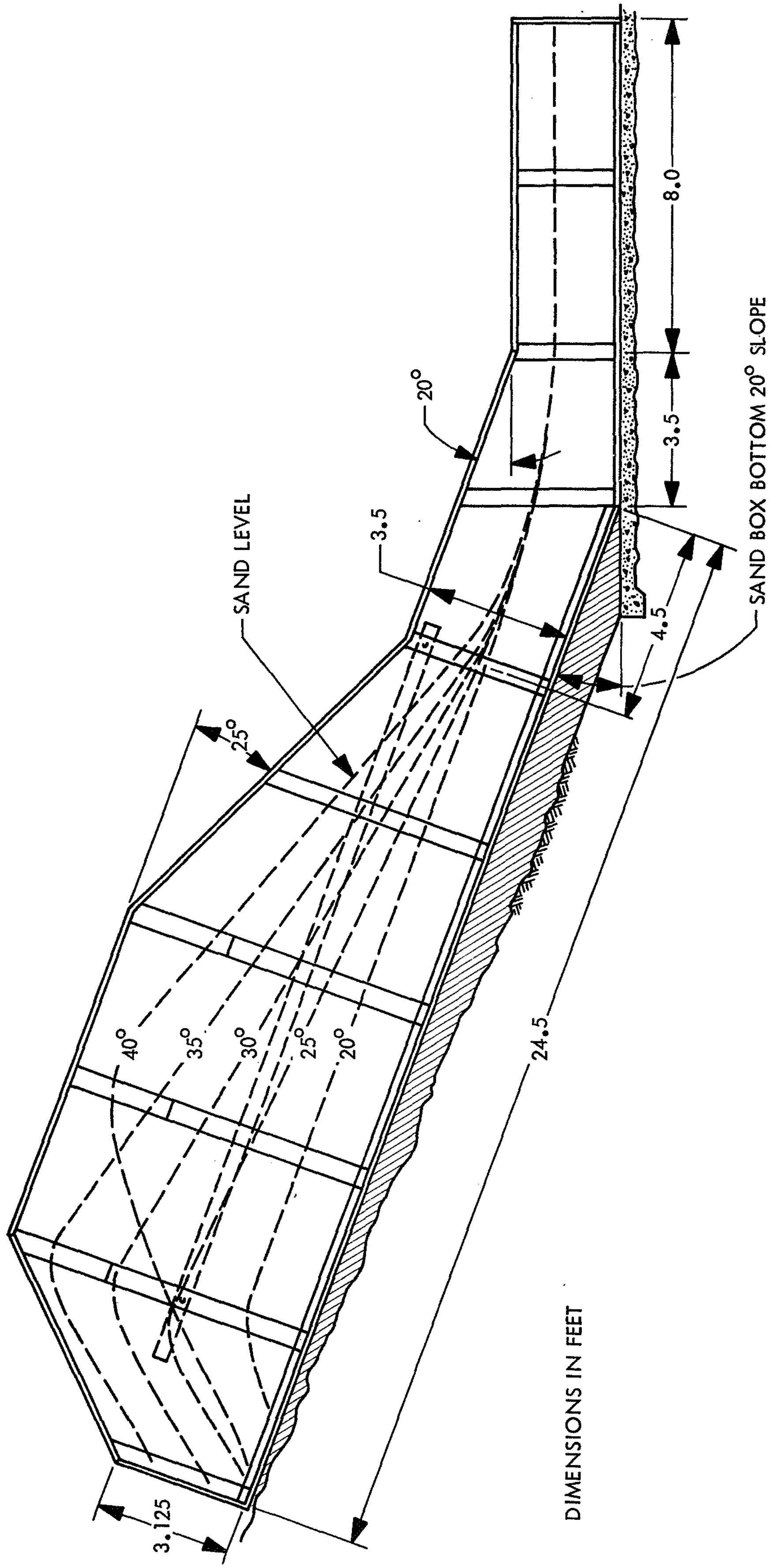

Fig. 1. Facility for Testing Vehicle Mobility on Soft Slopes (Plan)

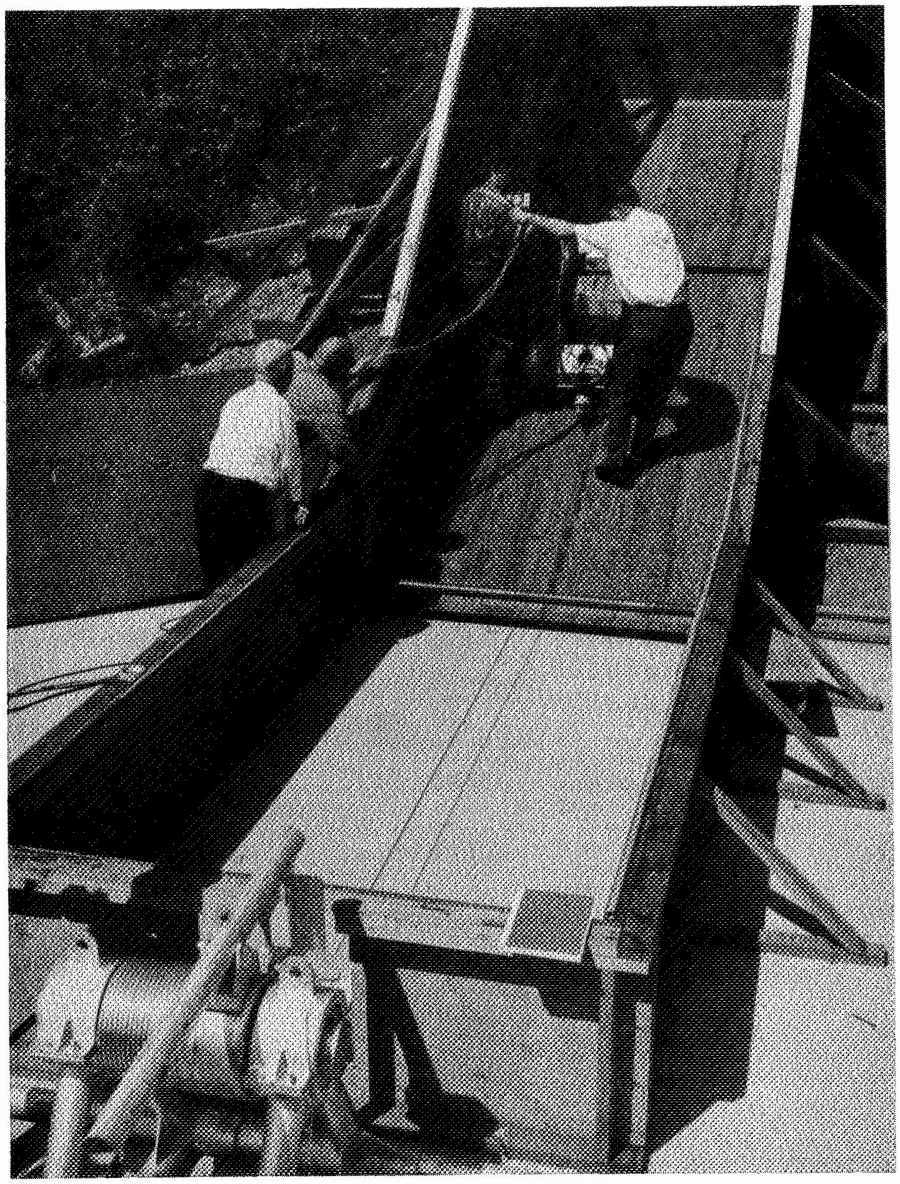

Fig. 2. Facility for Testing Vehicle Mobility on Soft Slopes

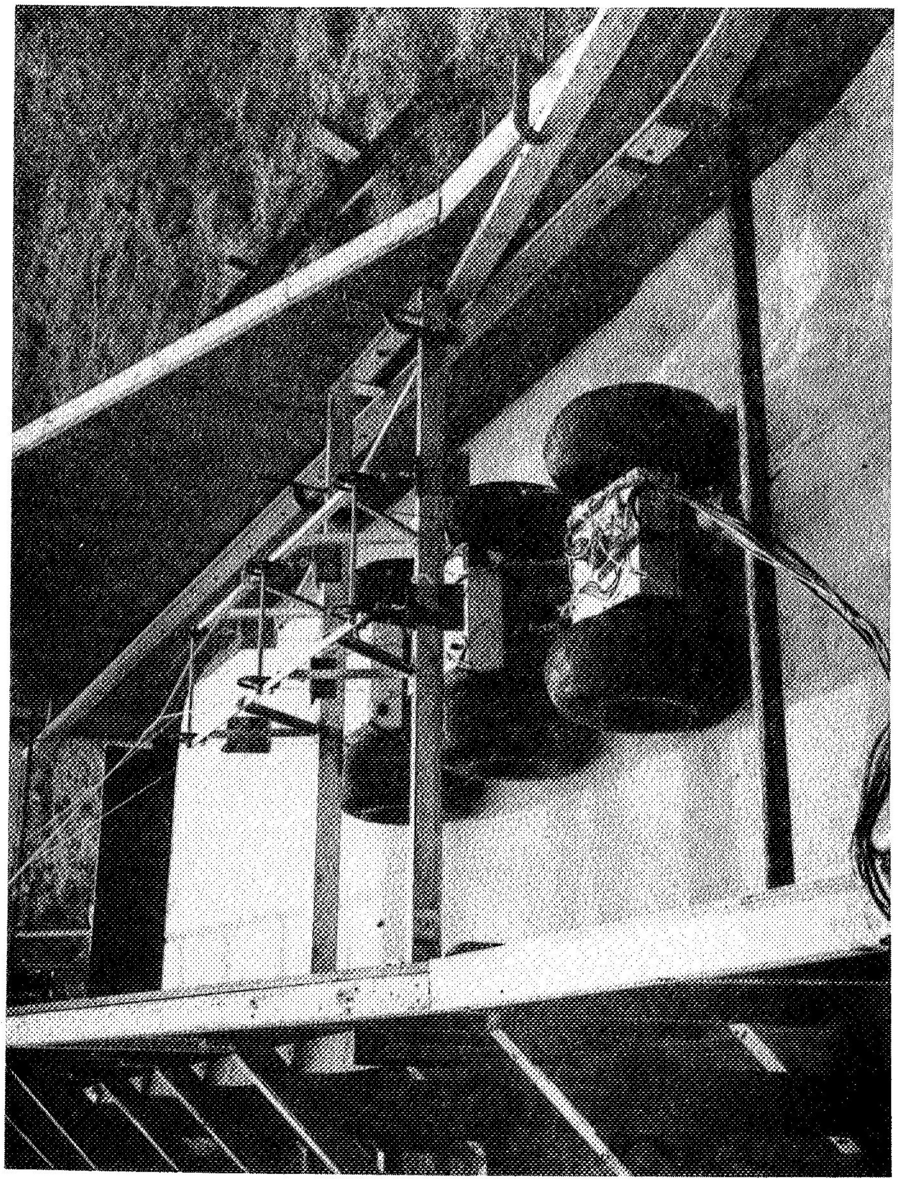

Fig. 3. Soil Bed of Vehicle Testing Facility

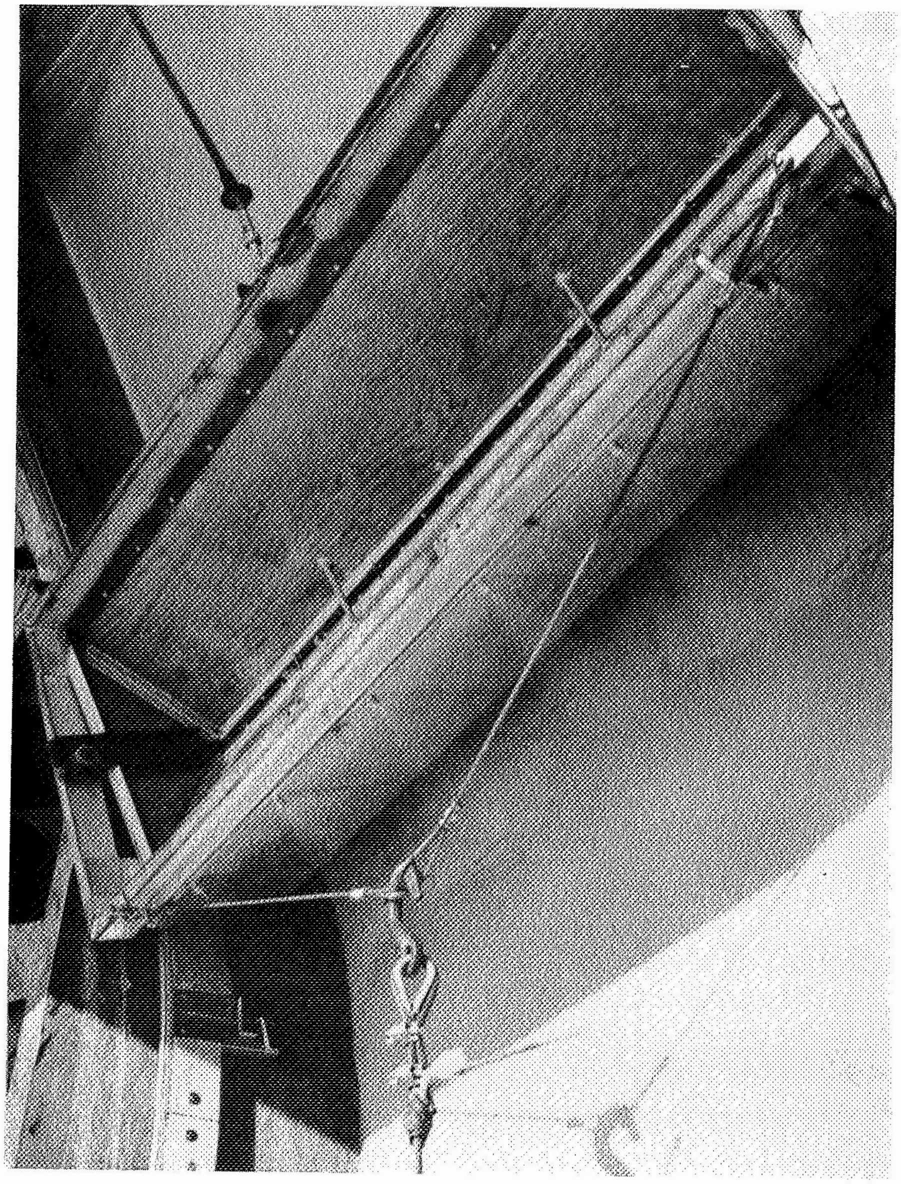

Fig. 4. Soil Hopper of Vehicle Testing Facility

The bottom of the hopper could be opened by means of a pin-spring supported gate which could be triggered open at any point along the soil track. Use of the hopper for spreading sand is shown in Fig. 5. When a sufficient depth of sand had been deposited, the soil surface was leveled off by means of a steel angle attached to the carriage frame in the manner suggested by the photograph, Fig. 6.

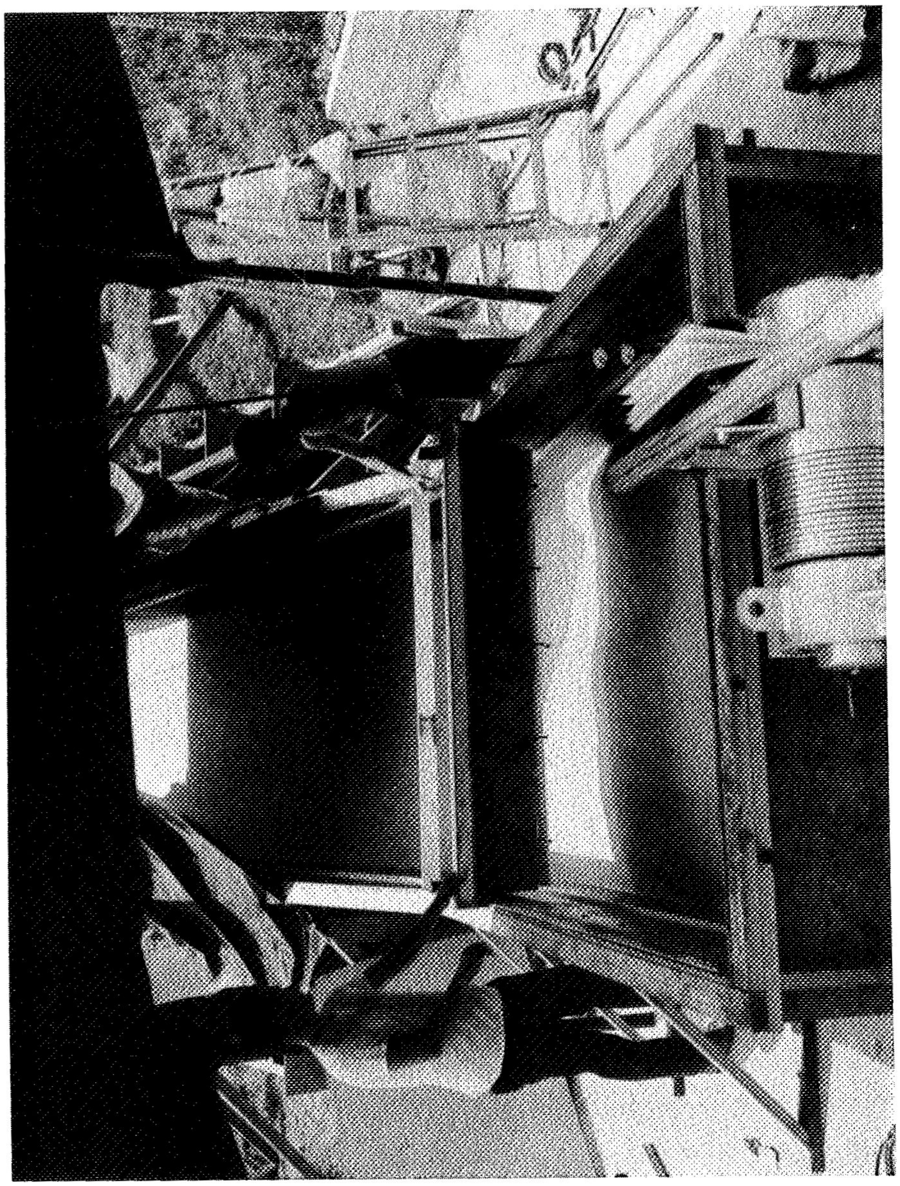

Fig. 5. Soil Hopper of Vehicle Testing Facility Spreading Sand

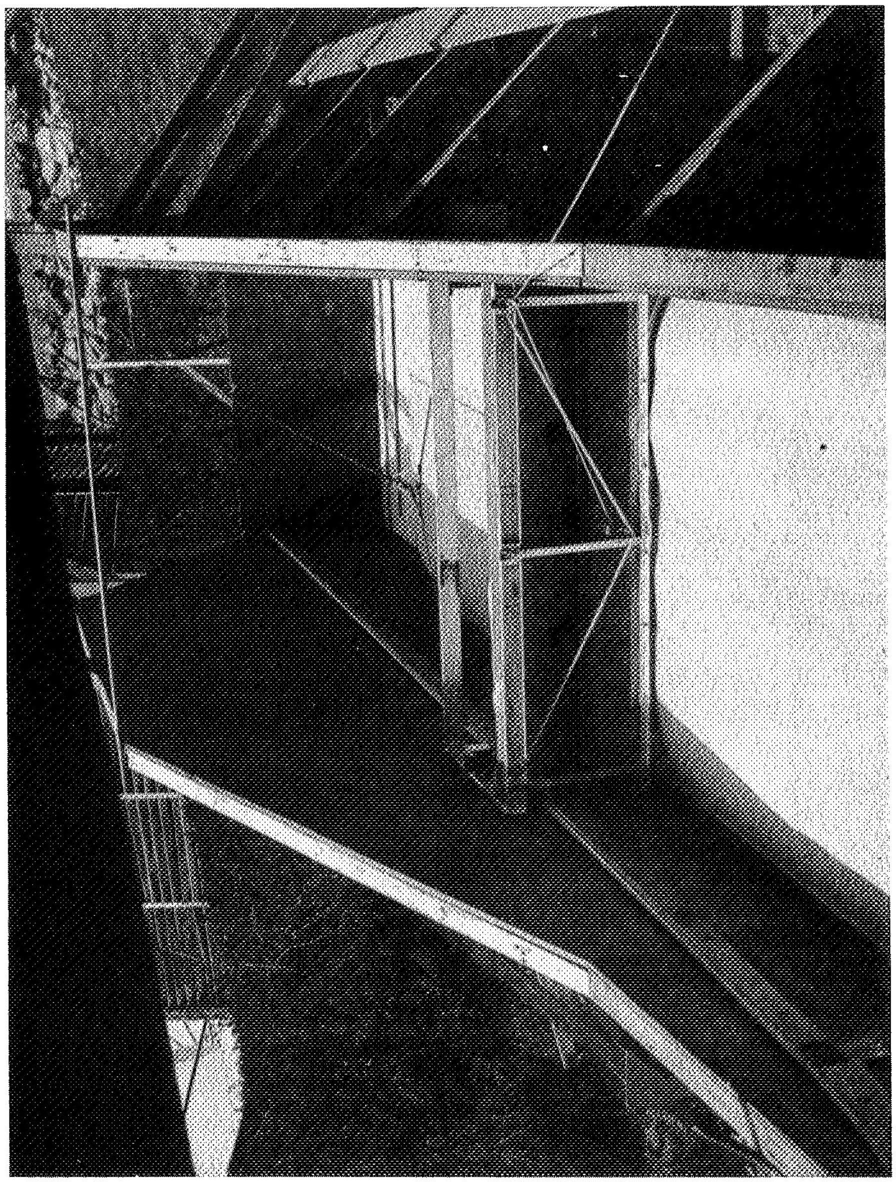

Fig. 6. Leveling of Soil Surface in Vehicle Testing Facility

V. TEST VEHICLE

The test vehicle used was the General Motors designed, Surveyor Lunar Roving Vehicle (SLRV). It has six wheels which have rubber covered tires of the pneumatic-wire reinforced type which were operated at a tire pressure less than 1/2 $lb/in.^2$ (Figs. 7, 8). The vehicle has no velocity control, and accordingly must be operated on a "stop-go" basis by remote radio control. Wheel rotation on the order of 15 rpm provided a movement of 70 ft/min over horizontal terrain. The vehicle was loaded onto the facility by means of the ramp, shown in Fig. 9, for a first run without sand on the bed. For subsequent runs with a prepared soil bed, the vehicle was carefully lifted and gently placed on the sand.

The photograph designated Fig. 10 is typical of the tests as the vehicle was about to climb the prepared soil bed slope. The photograph designated Fig. 11 is typical of the end of test run at the top of the slope.

Vehicle draw bar pull was measured parallel to ground support by means of a load cell connected at the rear end of the vehicle. The cell may be seen in all the figures showing the vehicle, and particularly in Fig. 9. Drag was applied by means of a braking arrangement shown in Fig. 12 and sketched in Fig. 13. The arrangement included a cable reel-up drum upon which the cable, attached to the vehicle through the load cell, could be wound. As it was unwound by movement of the vehicle, drag was exerted on the cable by means of the brake shoe arrangement resting upon a braking surface which is part of the drum construction. As shown in Fig. 13, the amount of drag could be varied by loading the drum by means of a pipe load arm and turnbuckle arrangement. Alternately, drag could be generated by weights contained in the pail which is shown hanging from the load arm.

Drag was applied parallel to the track surface by passing the cable beneath the roller which can be seen in Figs. 2, 3 and 10 and is sketched in Fig. 13. The position of the roller axis could be adjusted to match soil slope angle so that drag was applied parallel to the track surface. The means by which this was accomplished is indicated in Fig. 3.

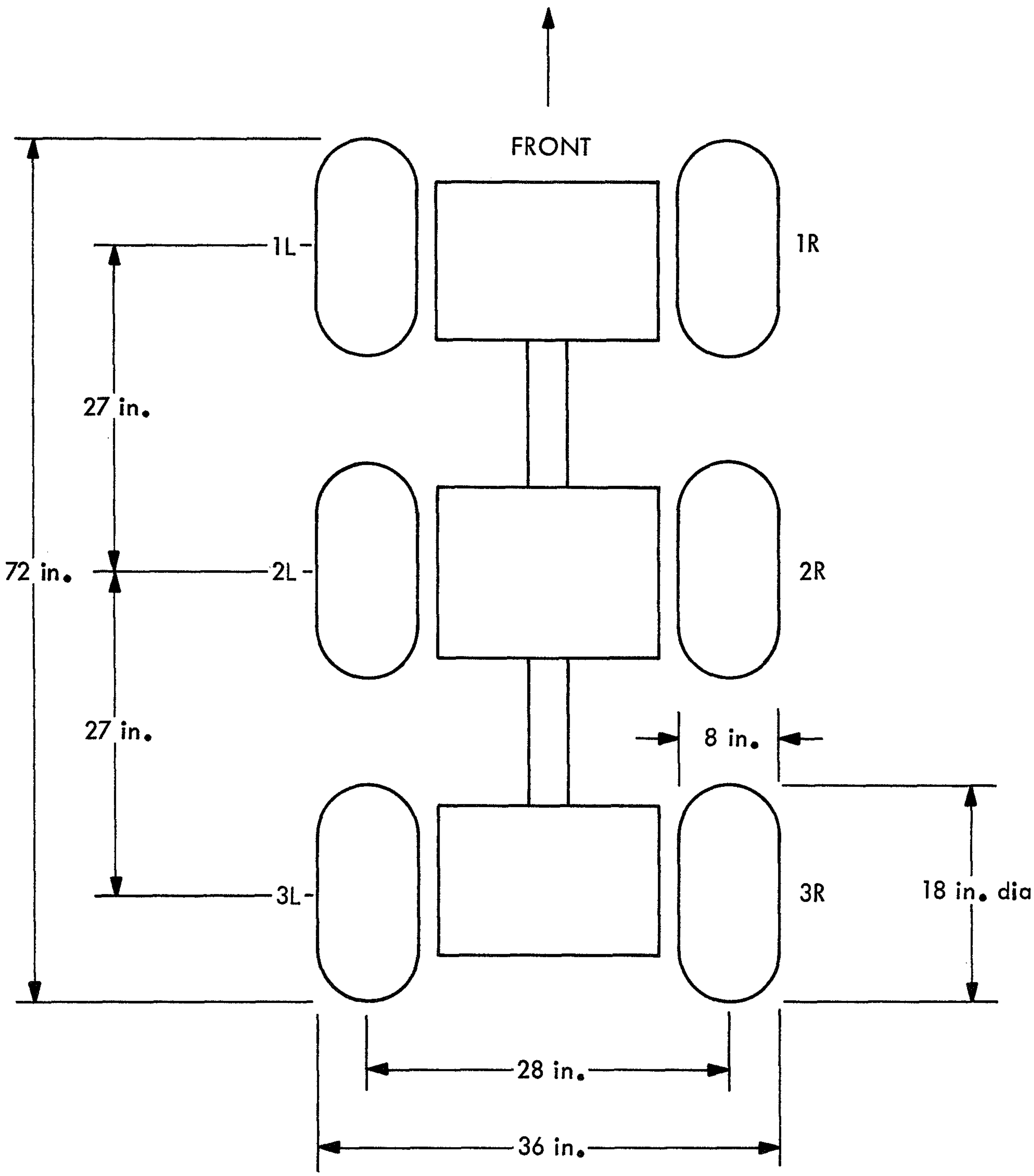

Fig. 7. SLRV Size Configuration (Plan)

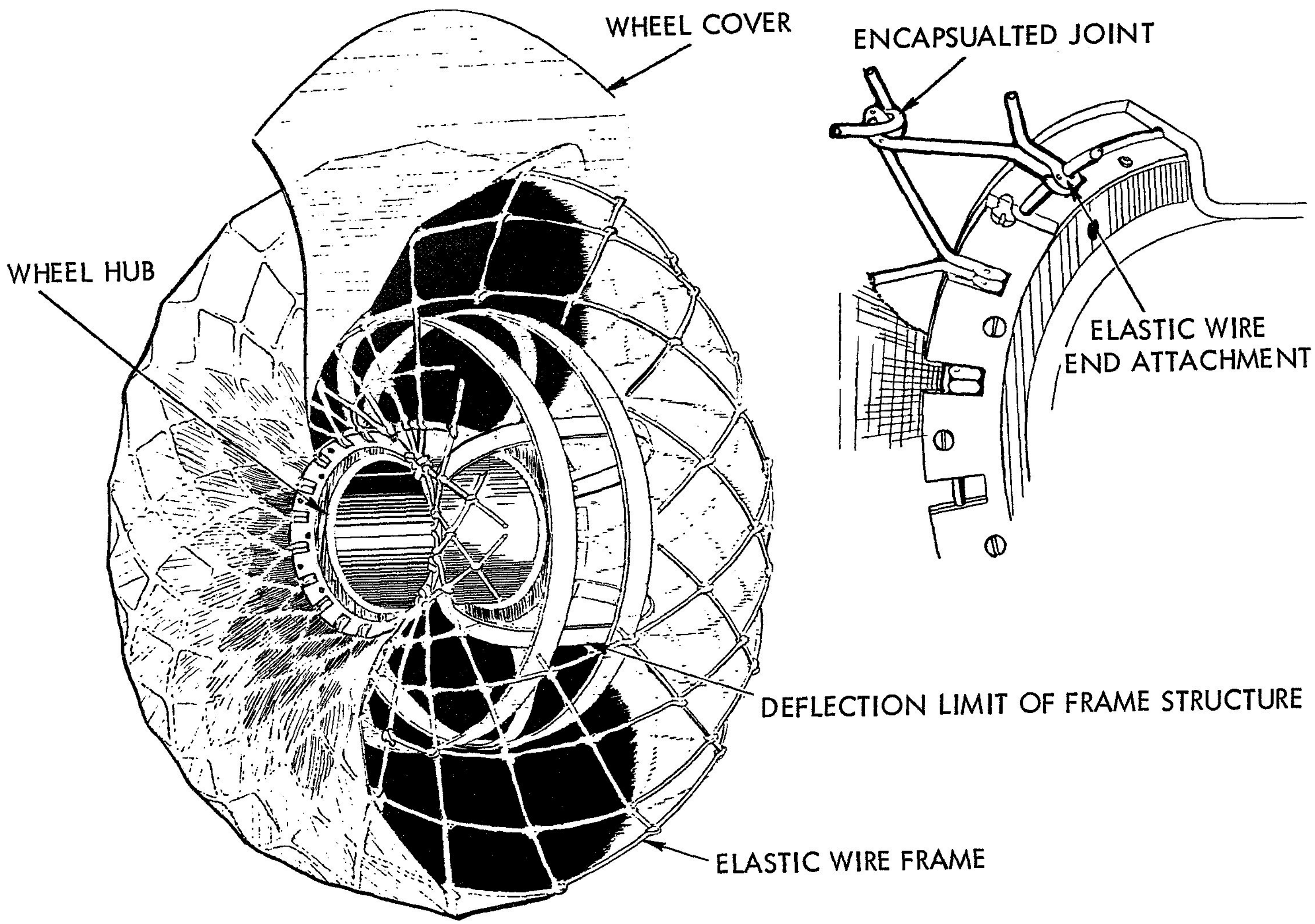

Fig. 8. Elastic Wheel

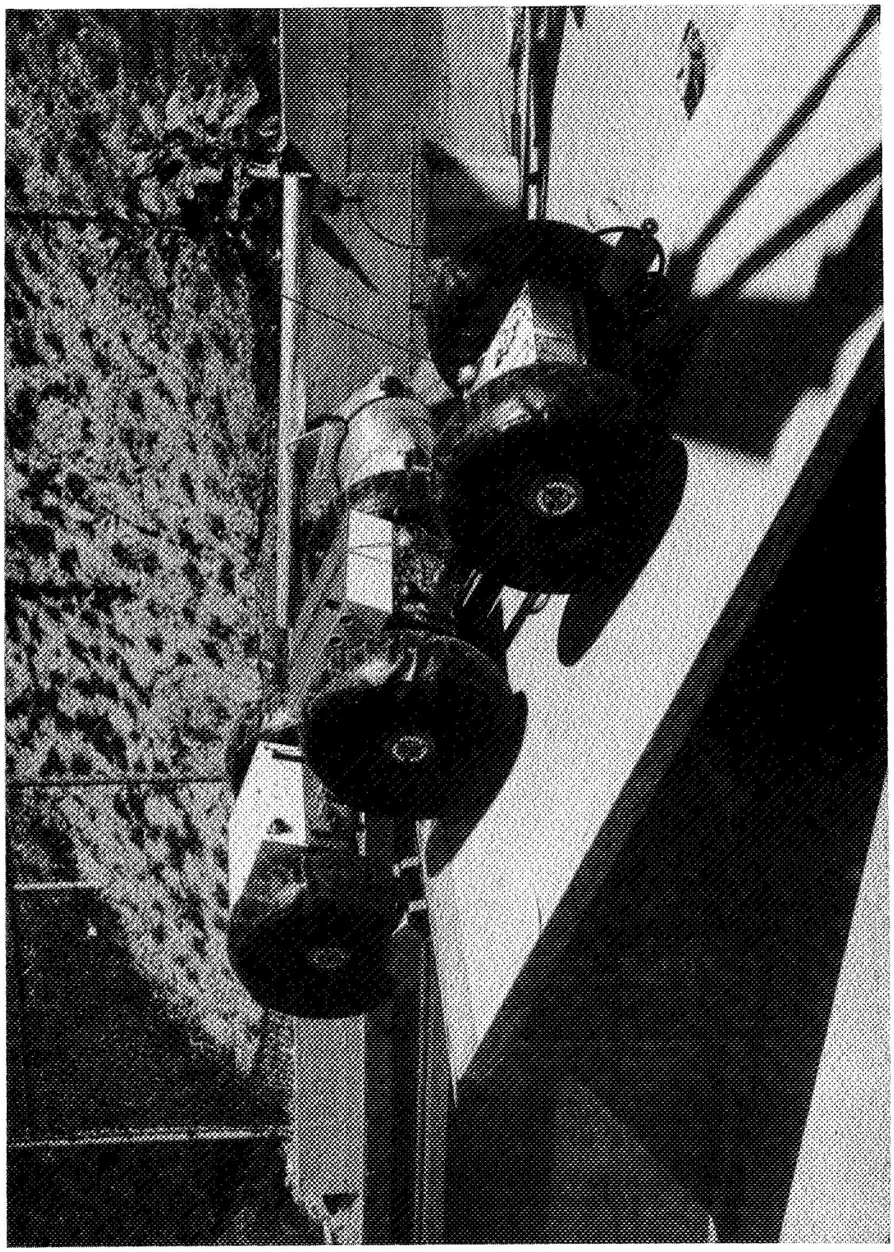

Fig. 9. Loading of SLRV onto Vehicle Testing Facility

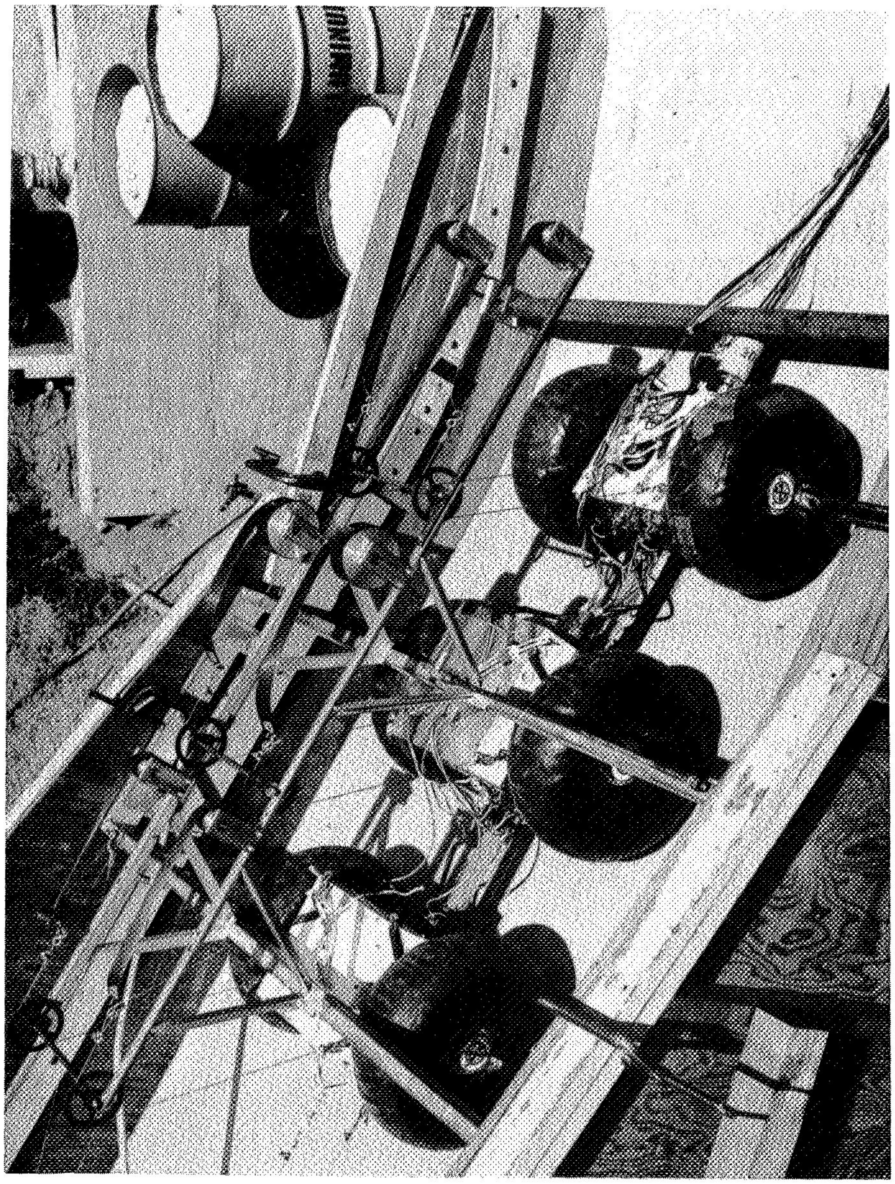

Fig. 10. Initializing the SLRV for Test Run

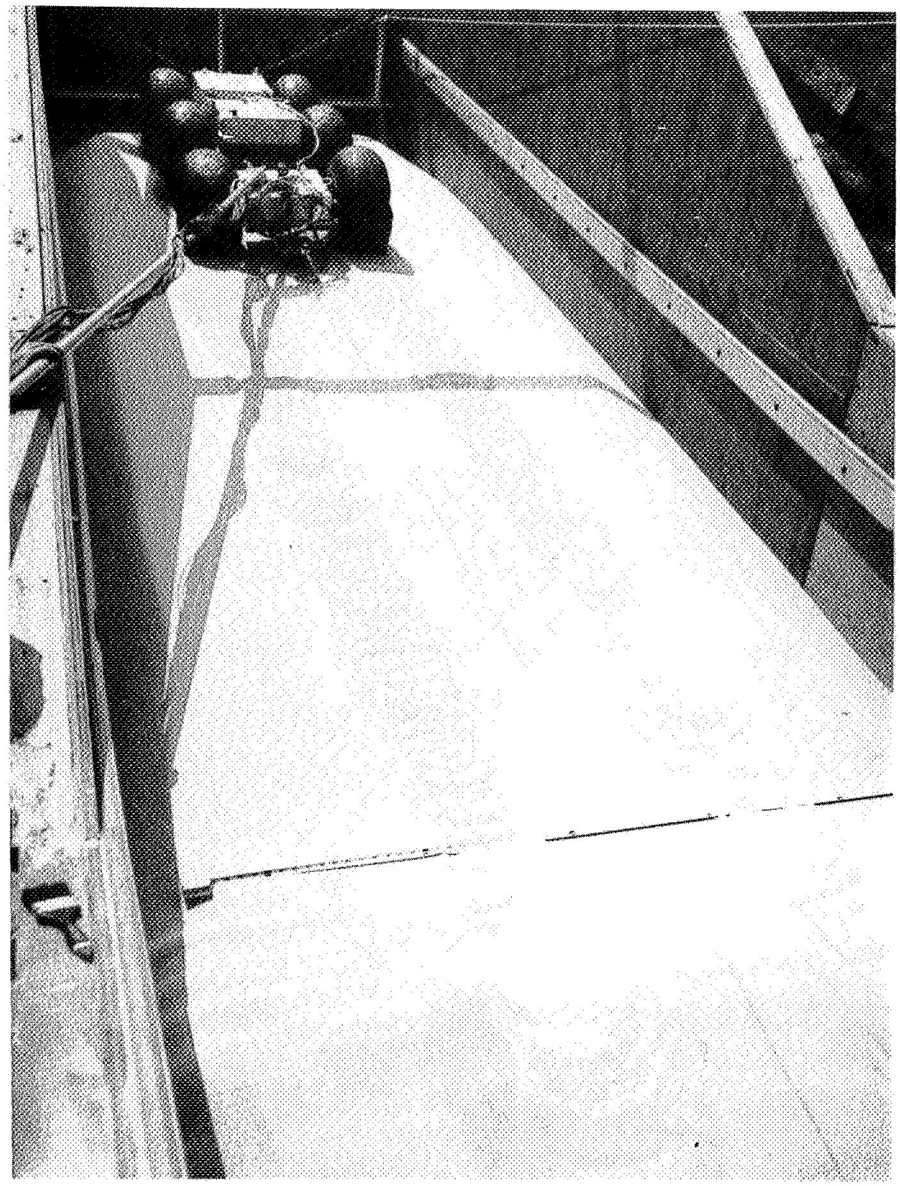

Fig. 11. SLRV at End of Test Run

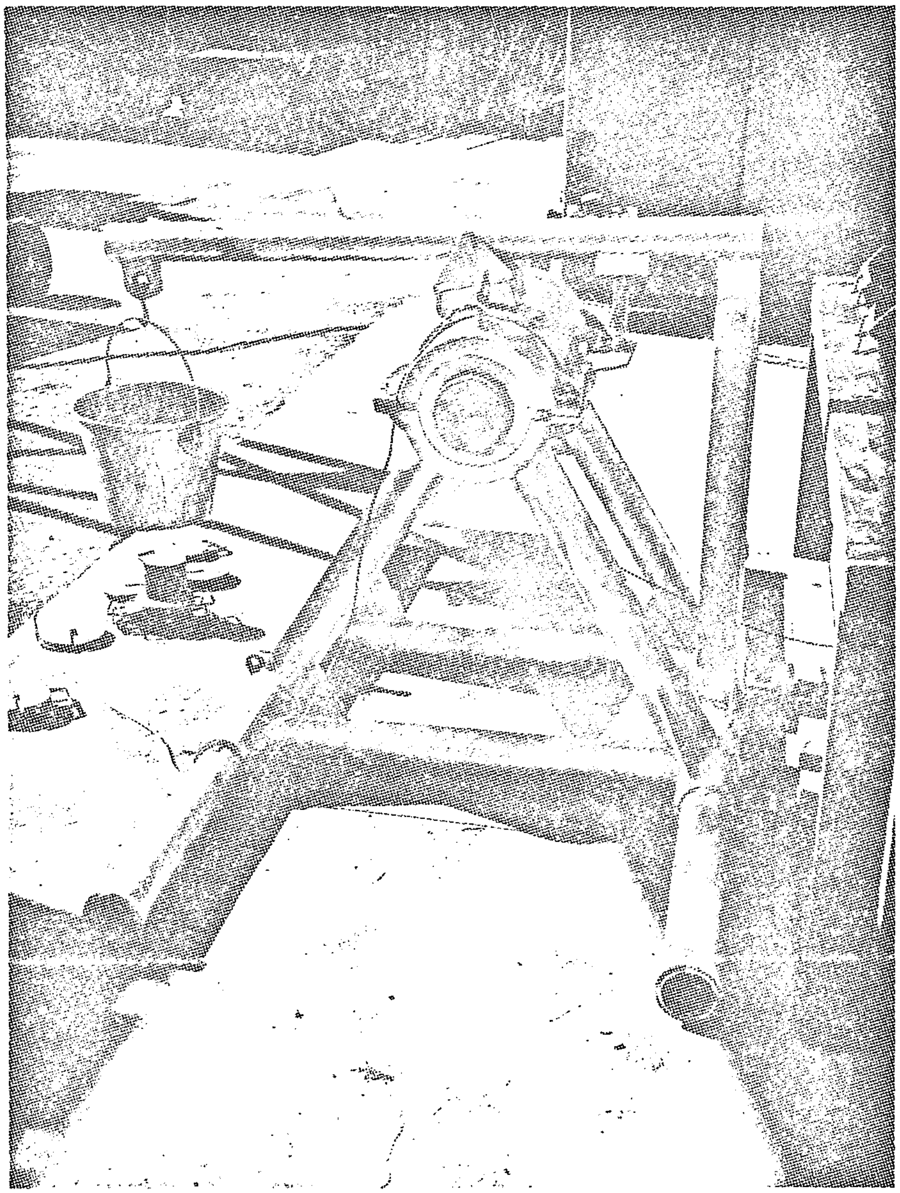

Fig. 12. Braking Arrangement of the Vehicle Testing Facility

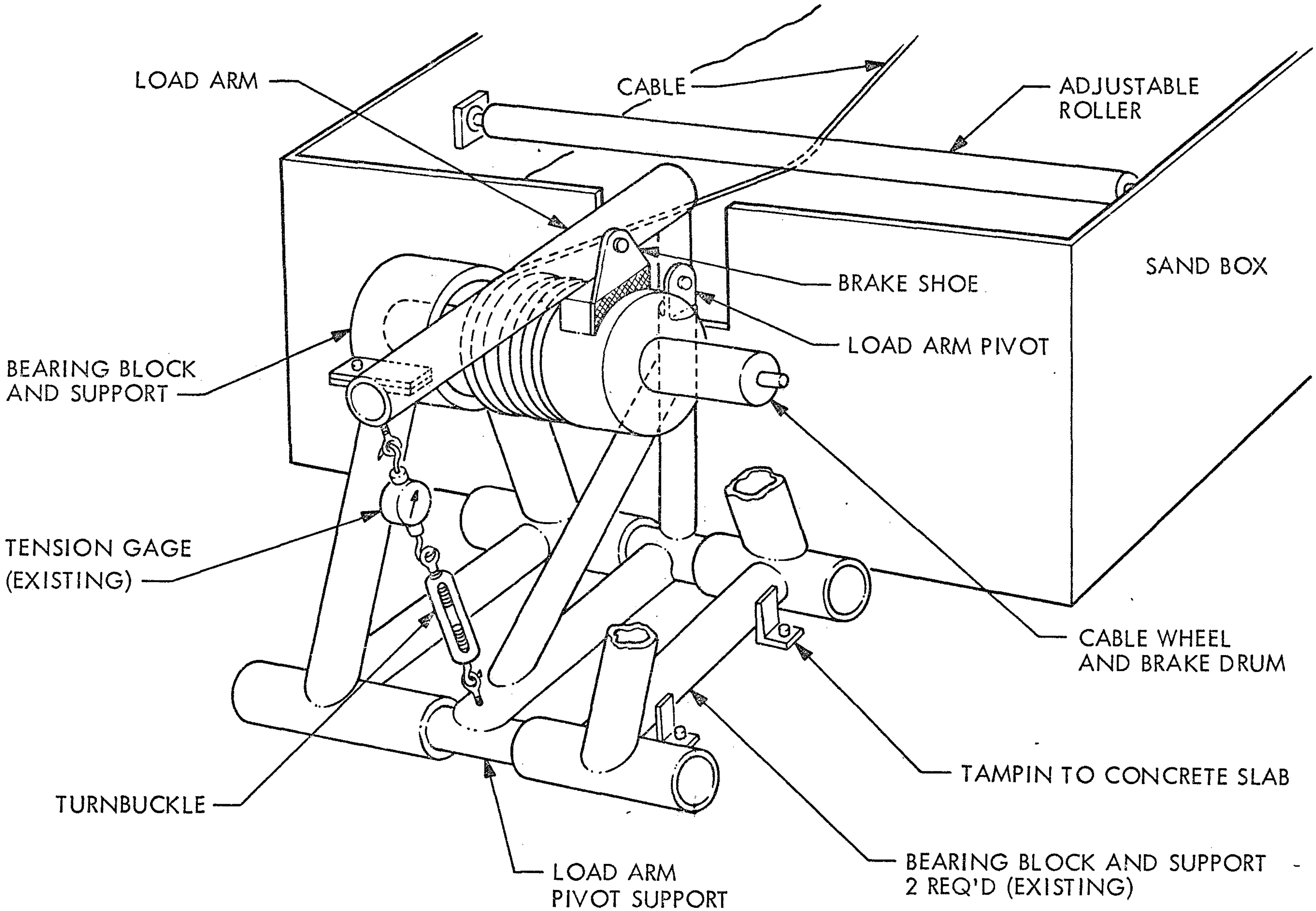

Fig. 13. Braking Arrangement of the Vehicle Testing Facility (Plan)

Some of the tests were made at full vehicle weight (158.4 lbs) and others at a reduced one-quarter vehicle weight in order to obtain approximate soil-wheel stress levels which may apply to lunar gravity conditions. Load lightening would be effected by two different arrangements. Figure 3 shows a system carried by the carriage frame in which load lightening was effected by counterbalancing weights applied to each wheel. A similar arrangement using negator springs[1] for the same purpose is shown in Fig. 10.

In order to obtain more accurate data with respect to vehicle performance, it was necessary to eliminate the effect of friction in the brake drag system, to balance out the effect of the downward component of the weight of the carriage frame, and to match the velocity of the carriage frame to that of the SLRV when the tests involving one-quarter vehicle weight were run.

This was accomplished by use of the counterweighting arrangements shown in Fig. 14. Brake drag and the frictional effect on the drag cable produced as it passed under the rollers was balanced out by using a counterweighted cable which passed over pulley A (Fig. 14) and attached to the front end of the vehicle. Initial adjustment was made without the vehicle. The counterweight was adjusted until the cable could be pushed in either direction by application of a very small force. This arrangement, when attached to the vehicle, was all that was needed for tests conducted at full vehicle weight.

For the one-quarter weight tests, a second counterweighting arrangement was used to offset the downward slope component of the weight of the carriage frame. Another counterweighted cable, passing over pulley B (Fig. 14), was attached to the forward end of the carriage frame. The counterweight was adjusted until the frame would move in either direction on application of a small force.

In order to maintain equal velocities for the SLRV and the carriage frame, marks or flags were placed on both cables and established in register. It was the duty of a technician to monitor the flags and to adjust carriage frame movement as necessary to maintain flag registration. Although the arrangement did not make it possible to maintain equal velocities on an absolute basis, it was possible to maintain equivalent velocities within acceptable limits.

---

[1] Provided by Ametek-Hunter.

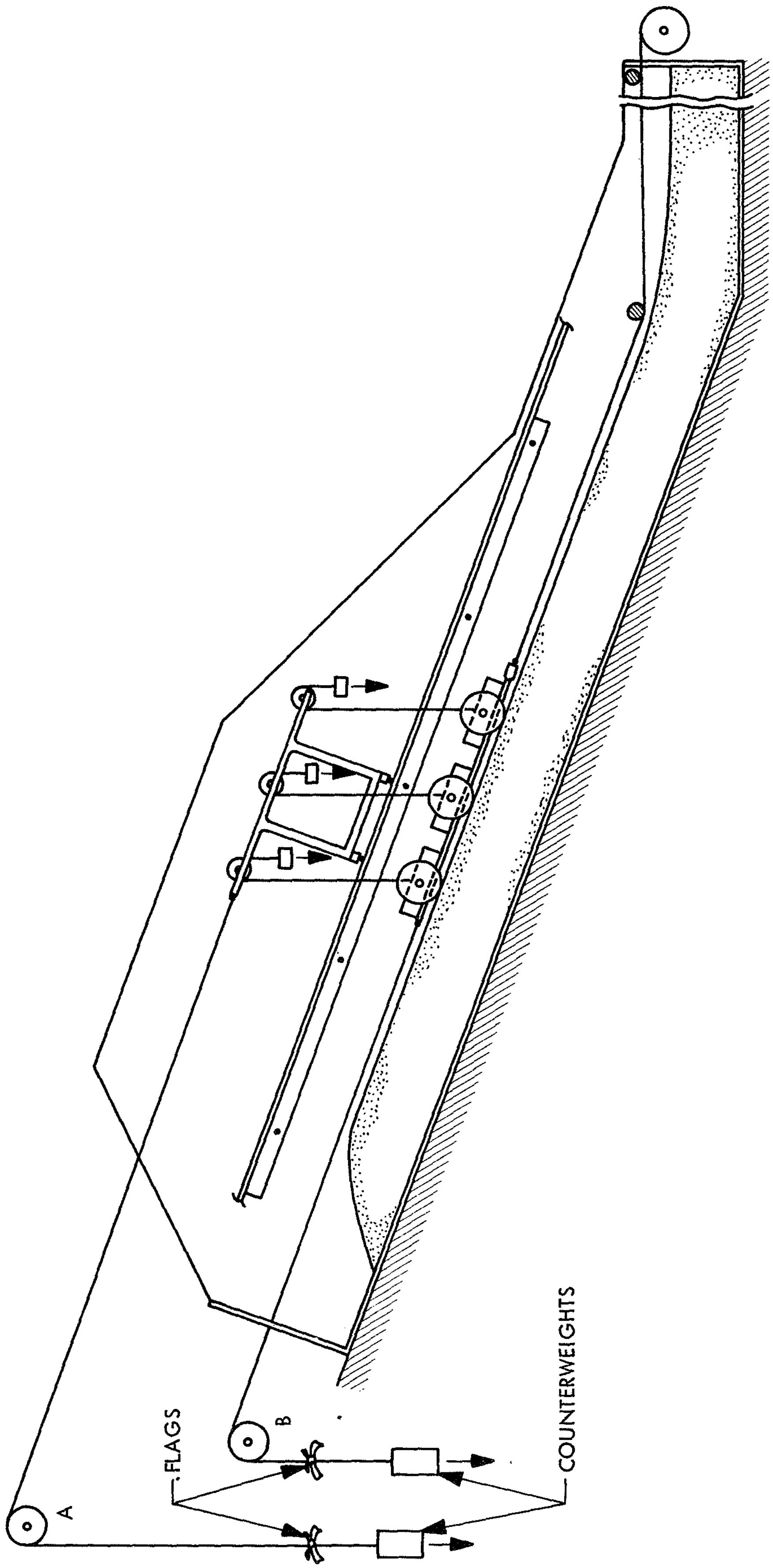

Fig. 14. Counterweighting Arrangement for Vehicle Testing Facility

VI. TEST MEASUREMENTS

Table 2 indicates some basic SLRV drive system values and soil-tire measurements.

Wheel torque /current measurements covered the expected torque operational levels as shown in Fig. 15. As noted, wheel motor responses are dissimilar in both their torque/current ratios and angular velocities. Lack of uniformity in vehicle axle load distribution produced slight differences in the effective rolling radius and corresponding tire deflections. The three right side wheels turn proportionally faster than the left side wheels, and the vehicle has a tendency to steer to the left, but proper initial vehicle orientation and control permitted the SLRV to maintain its position within the middle third of the track.

In order to minimize the soil-tire contact stresses, it was decided to increase the contact imprint area. Therefore, the tire inflation pressure was reduced to the ones shown in Table 2, Column (e). Since wheel slip values and axle loads are not uniform, these factors produce slight slip differences between wheels. On an average, drawbar pull and wheel torque values are considered in terms of a single slip number for the whole vehicle. Soil contact pressures were estimated from tire imprints on the undisturbed soil bed as shown in Fig. 16. The beaded appearance is due to the soil-tire compliance at the soil contact interface. The estimated contact pressures are shown in Table 2, Columns (e) and (f).

No definite single sinkage values can be assigned for light soil-tire contact pressures, as is normally done for large loads, and in the test analysis, sinkage was not considered to constitute a controlling parameter.

The vehicle was set gently on the soil track. All tests started from zero velocity at the corresponding slope. The numerical analysis refers to a time interval when the vehicle reaches a steady state condition in the pull force, wheel torques, and velocity levels.

TABLE 2. SLRV DRIVE SYSTEM AND TIRE MEASUREMENTS

Wheels*	(a) Torque current, in. -lb/amp	(b) Axle loads, lbs	(c) Equiv. rolling radius (R_e), in.	(d) Tire deflect, in.	(e) Inflat. press., lb/in.^{2}	(f) Soil-Tire contact press., lb/in.^{2}	(g) Soil-Tire contact press., lb/in.^{2}	(h) Angular veloc. rad/sec	(i) Wheels relative veloc.
1L	132	29.30	8.09	1.125	0.20	0.727	0.3775	1.441	1.00
1R	109	28.40	7.88	2.250	0.20	0.609	0.365	1.685	1.17
2L	102	17.22	7.85	1.125	0.10	0.463	0.284	1.718	1.20
2R	106	16.72	7.85	1.625	0.10	0.378	0.220	1.653	1.15
3L	126	31.65	8.00	1.500	0.30	0.602	0.442	1.500	1.04
3R	118	30.74	8.00	1.625	0.30	0.628	0.396	1.595	1.11

*1, 2, 3 refers to front, middle and rear axles; L = Left, R = Right

Notes for Table 2:

(a) Motor type globe, 102 A 209-9, see Fig. 15.

(b) Approximate axle loads distribution obtained using fish-scale of 0-60 lb range.

(c) Equivalent flexible wheel rolling radius (R_e) estimate is based on SLRV mobility on hard asphalt surface and a tire inflation pressure of 1/2 lb/in.^{2}

(d) Static conditions corresponding to inflation pressure according to (e).

(e) Minimum pressures required to stabilize wheel wire mesh.

(f) Based on inflation pressure of 0.50 lb/in.^{2} for all tires, Fig. 16.

(g) Inflation pressure - 0 lb/in.^{2} (wheel supported by wire mesh only).

(h) Unloaded wheel condition.

(i) Wheel relative velocity relates to Wheel 1L.

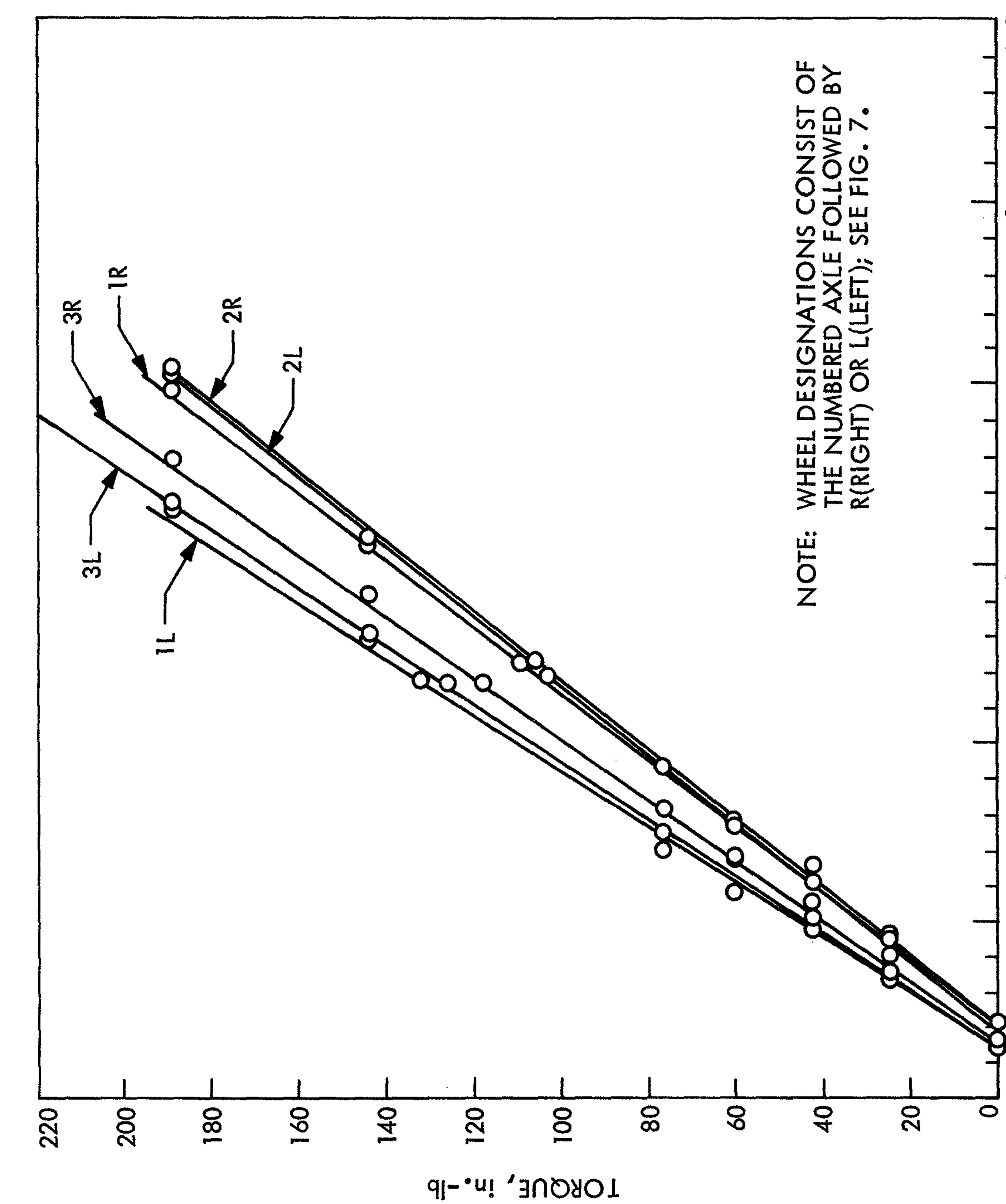

Fig. 15. Wheel Motor Torque - Current Tests

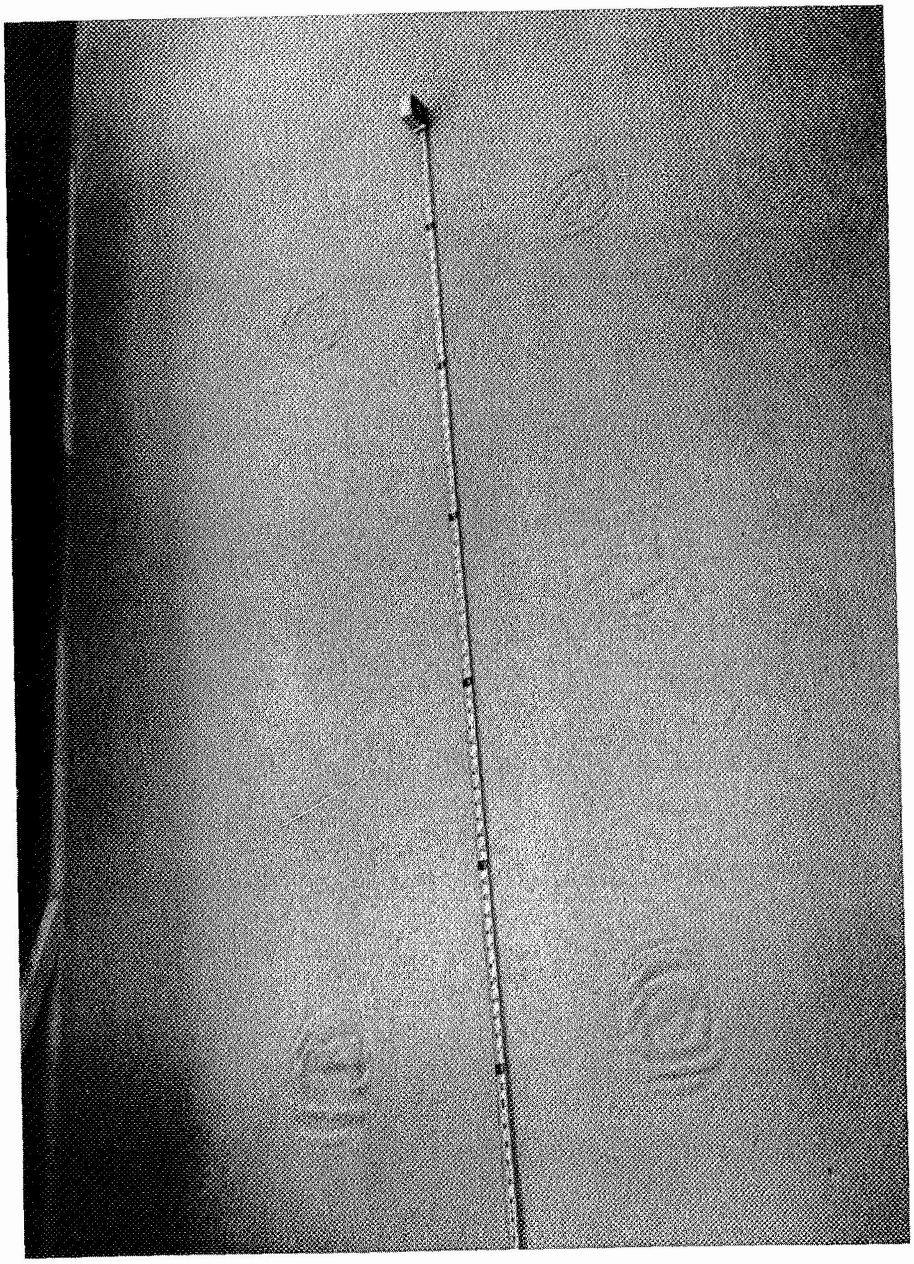

Fig. 16. Soil-Tire Imprints

VII. INSTRUMENTATION

Test measurements consisted of graphical and/or magnetic recordings of the vehicle drawbar pull, vehicle velocity, velocity of each wheel, wheel motor currents, and battery terminal voltage. All measurements were time-related by suitable indications on the instrumentation records.

The velocity of each wheel is measured by a fixed magnetic pick-up (air-Pax 340-0006) on each axle. Sixteen small magnets are cemented to a 4 in. diameter aluminum plate mounted on the inside of the hub of each wheel. The magnets are equally spaced on the plate at 22-1/2 deg. The stationary pick-ups on the axles are on a radius of 1-15/16 ins. The velocity is computed by measuring the time between pulses coming out of the magnetic pick-up.

Wheel currents are measured by reading the voltage across shunts that are in series with each wheel motor.

Vehicle velocity is measured with a DC tachometer (Bechman 9150) coupled to the wire drum. (The ratio of drum diameter to tach shaft diameter is 11.66. Maximum tachometer rpm is calculated to be no more than 250 rpm with no restraint on the vehicle.)

Total drawbar pull load is measured by bolting a load cell (Aliner 342, 200 lbs) to the rear of the vehicle axles by means of an under carriage aluminum bracket.

Total current and battery voltage come from an internal shunt and across the battery respectively.

These parameters were recorded on an oscillograph (Midwestern 603) using light sensitive paper. A flat frequency response of 90 cycles (±5 percent) was obtained by using 150 cycle galvanometers. Paper speed was run at between 1 and 2 in./sec. Five cycle square wave timing signal was put on each side of the paper to give 100 millisecond time.

Along with the oscillograph, an Ampex FR1300 tape recorder registered wheel velocities, wheel currents, and vehicle velocity on 1 in. magnetic tape. This recorder was run at 7-1/2 in./sec giving an overall frequency response of DC to 2.5 kHz.

VIII. LABORATORY TESTS OF SOIL MECHANICAL PROPERTIES

Typically, the soil bed consists of medium to fine white silica sand. The grain size distribution curve is given in Fig. 17. Sand is poured from the hopper at a constant rate from a variable height of 6 to 24 in. through an adjustable opening which was held at a constant 0.10 in. width. This produces a soil bed with the density increasing linearly with depth.

Some of the tests involved slightly cohesive soil produced by wetting the sand. This was accomplished by a set of water jet spraying devices mounted on the uphill end of the hopper which were activated after or during sand deposit. The arrangement can be seen in part in Fig. 4. It required a fine spray distributor, hose reel, spring take-up, valves and connectors which were readily assembled into a suitable system.

A. DRAINED DIRECT SHEAR TESTS ON MIXED SILICA SAND

The purposes of these tests were to determine the cohesion of the wet mixed silica sand used for the SLRV tests and to establish the possible difference between the internal friction angles of the wet and dry mixed silica sand having the same dry density.

To insure the homogeneity of the testing sample, the latter was prepared in three layers. The density of the layered soil was controlled by the same amount of vibration. In order to wet the samples, a porous stone was set on the top of each sample and sprayed with water until water drained freely out of the outlet. Due to the high permeability of the sand sample, the consolidation process was assumed to be completed in 15 minutes. With a slow moving motor, the direct shear tests were conducted under strain-controlled conditions without producing any excessive pore water pressure.

Four tests were conducted for each normal load. Since each sample had different density and water content, the data was interpolated in order to arrive at a density of 1.628 gr/cc (101 lb/ft^3) and water content of about 19.5 percent, as used for the vehicle tests. Direct shear test results for dry and wet silica sand are shown in Fig. 18.

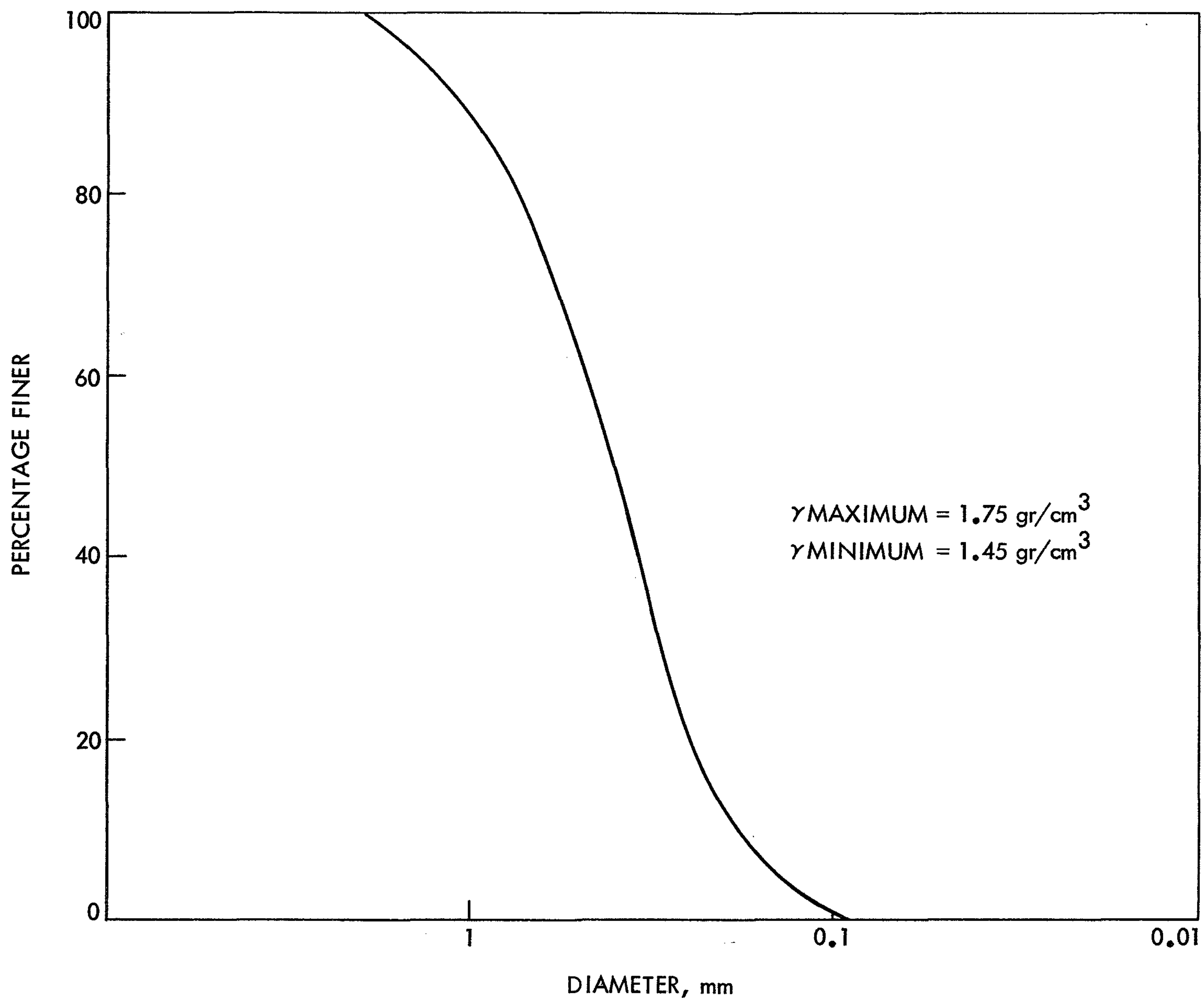

Fig. 17. Grain Size Distribution - Medium to Fine White Silica Sand

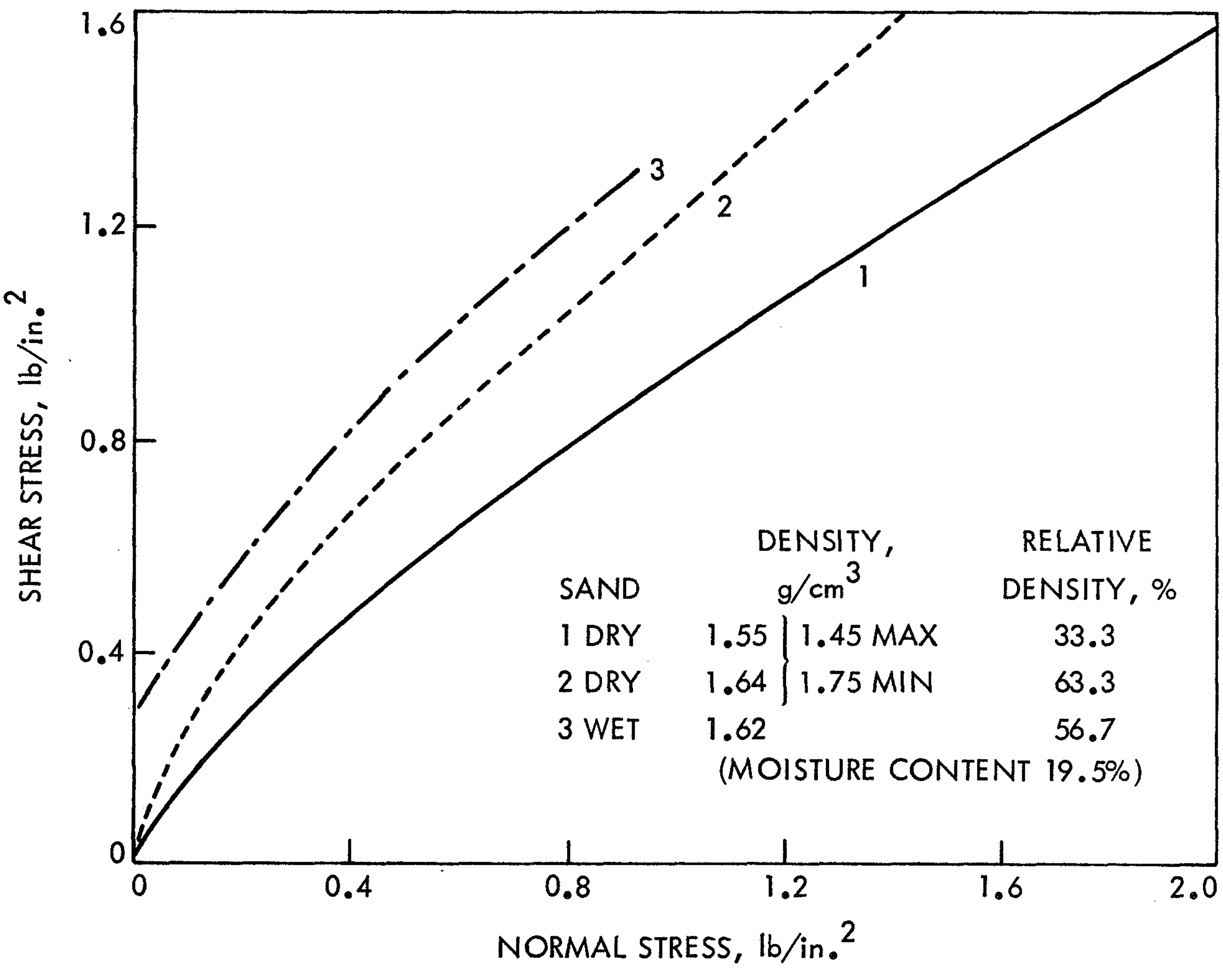

Fig. 18. Direct Shear Tests - Dry and Wet;
Medium to Fine Silica Sand

B. SOIL ANGLE OF REPOSE

Soil samples were carefully prepared inside a 4 x 6 x 12 in. wooden box. The top of the level surface of the soil sample coincided with the level of the top edges of the box. The box was hinged at one end. Gradually the soil box was tilted until a stream of soil particles started to flow down. The inclination of the box was then taken to be the angle of repose of the soil sample, Fig. 19.

The tangent of the angle of repose varies more or less linearly with the relative density of the soil, Fig. 20. This is generally true for a cohesionless soil material.

C. SOIL SHEAR RESISTANCE TESTS ON SURFACE SLOPES

In order to gain some insight into soil-wheel mobility performance on slopes as related to the soil mechanical properties, the following basic aspects were considered: (a) the influence of plate-soil material properties, (b) the surface slope shear stress orientation, and (c) the lateral soil confinement on slope plate shearing strength.

Use was made of a test box with inside dimensions of 4 x 6 x 12 in. containing silica sand. The testing set-up is shown in Fig. 21. A loading plate transmits the load to the soil. A smooth wire, with one end attached to the loading plate and a bucket hung to the other, transmits the shear force. A pulley provides support and orientation of the shear force which is maintained parallel to the slope. The shear force is increased by a slow addition of lead shots at a constant rate into the bucket until shear failure is reached. Two types of plate shearing surfaces were used:

(1) Sand Layer Shearing Surface: A thin layer of sand particles attached on an aluminum plate face by means of an adhesive spray material.

(2) Rubber Shearing Surface: A 1/8 in. thick, flat neoprene rubber layer attached to the plate surface.

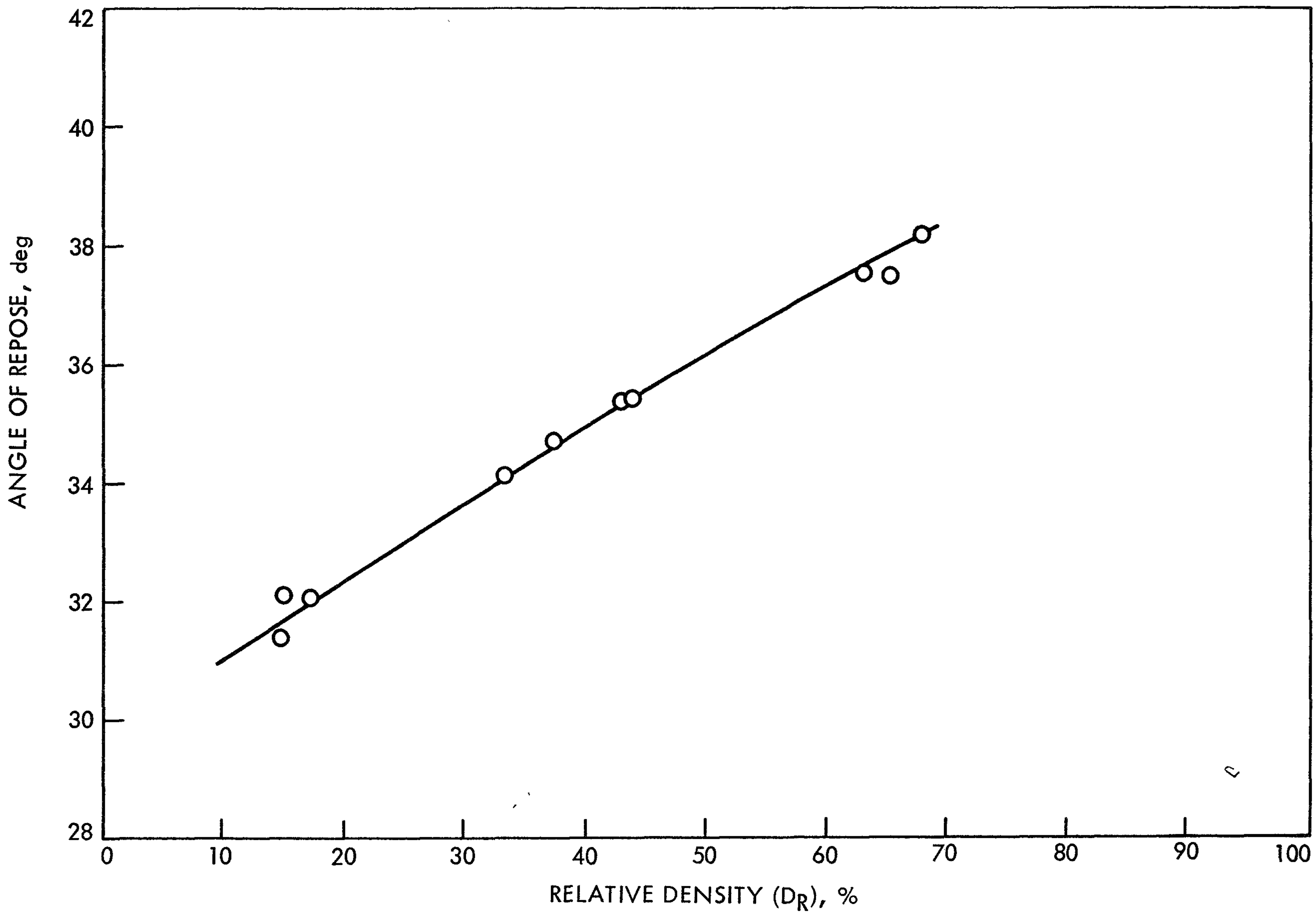

Fig. 19. Angle of Repose Versus Relative Density

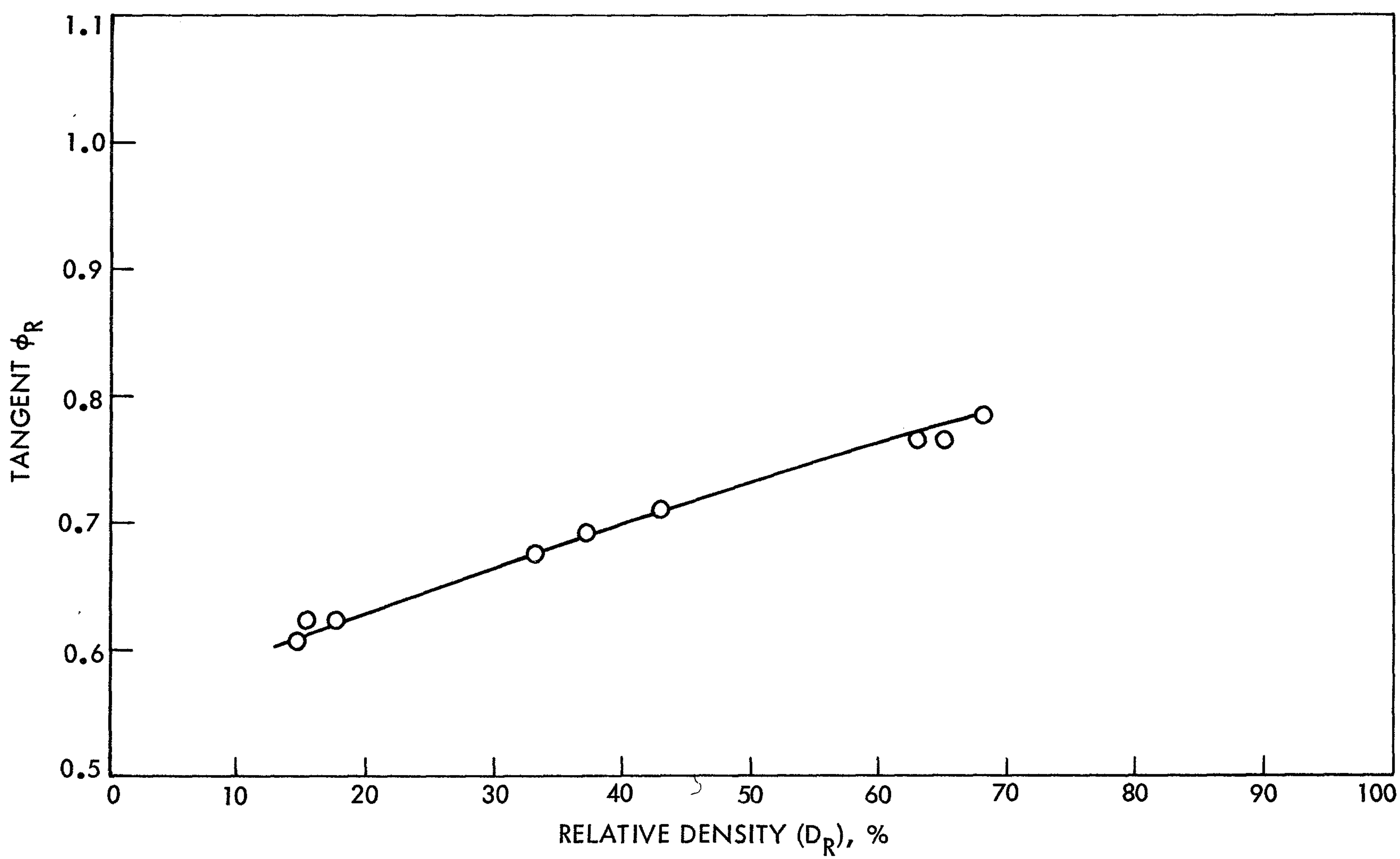

Fig. 20. Plot of Tangent of ϕ_R (angle of repose) Versus Relative Density, D_R

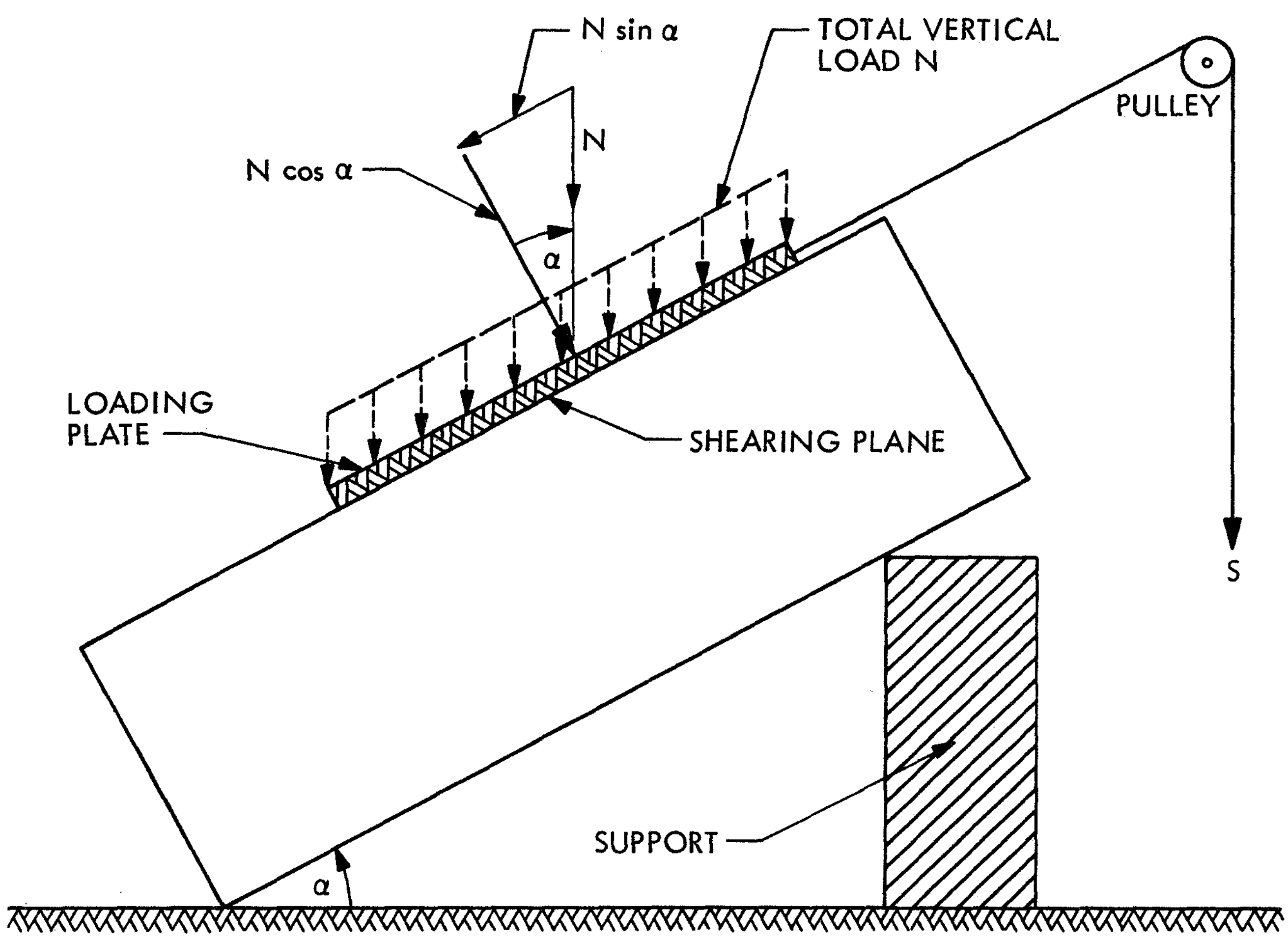

Fig. 21. Surface Shear Test Set-Up

Soil confinement ratio, C, is defined as the relative magnitude of the plate lateral normal pressure with respect to the total plate normal pressure:

$$C = \frac{\gamma z \cos\alpha}{\gamma z \cos\alpha + p_n};$$

γ = soil density, z = height of overburden from shearing surface,

α = slope angle and p_n = normal pressure.

The surcharge load is provided by adding soil of density, γ, to a height, z, above the shearing surface.

Based on these shear plate tests, the following observations and conclusions are derived:

(1) For any slope and using a sanded face material, the normal pressure versus the shear stress curve always shows a slight downward concavity at low normal pressures ($\sigma < 0.20$ lb/in.^{2}). Figures 22 to 24 indicate that the lower the applied contact pressure the larger the mobilized soil angle of internal friction. This behavior is due mainly to the predominance of shear strength derived from granular interlocking at the sanded plate face. It constitutes a favorable condition; entailing the development of proportionally higher soil thrust with reduced values of wheel-soil contact pressure.

(2) For a rubber (neoprene) plate the shear-normal stress performance on surface slopes is practically linear and independent of the level of applied pressure (Figs. 25 to 27). As it occurs for the rough sanded plate surface, no significant increase of shear strength is noted due lack of interface grain interlocking.

(3) Two well known facts are verified. The mobilized soil plate interface shearing resistance varies with the nature of the shearing surface. The sanded plate surface yields higher shear resistance than that of a rubber surface. The difference is about 15 percent and mainly concerns the larger interface roughness of the plate with the sand layer (see Figs. 28 and 29, at C = 0). Also, the shear strength of the slope surface increases with the increase of the soil relative density.

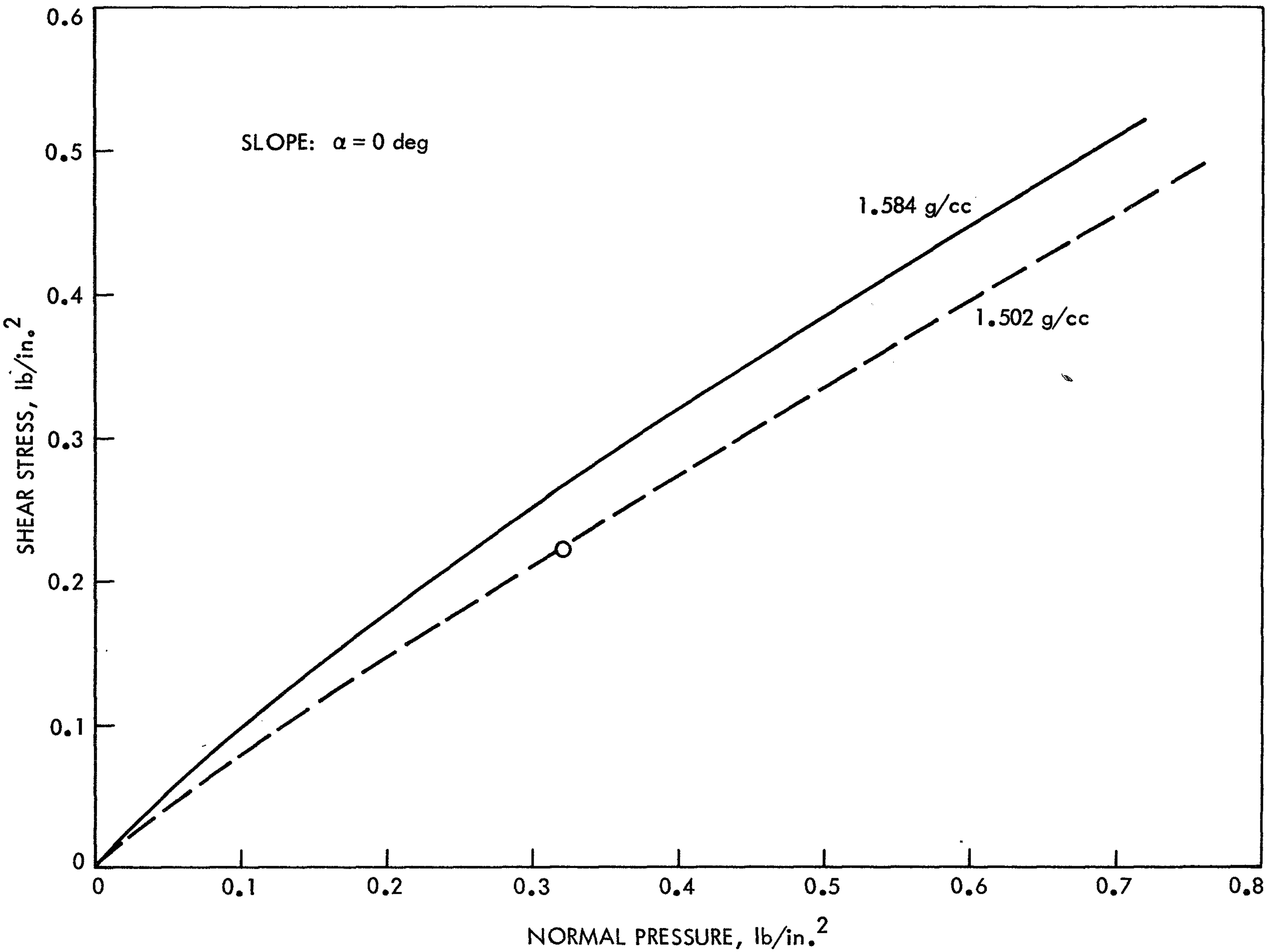

Fig. 22. Sandy Shearing Plate on Soil - Level Surface

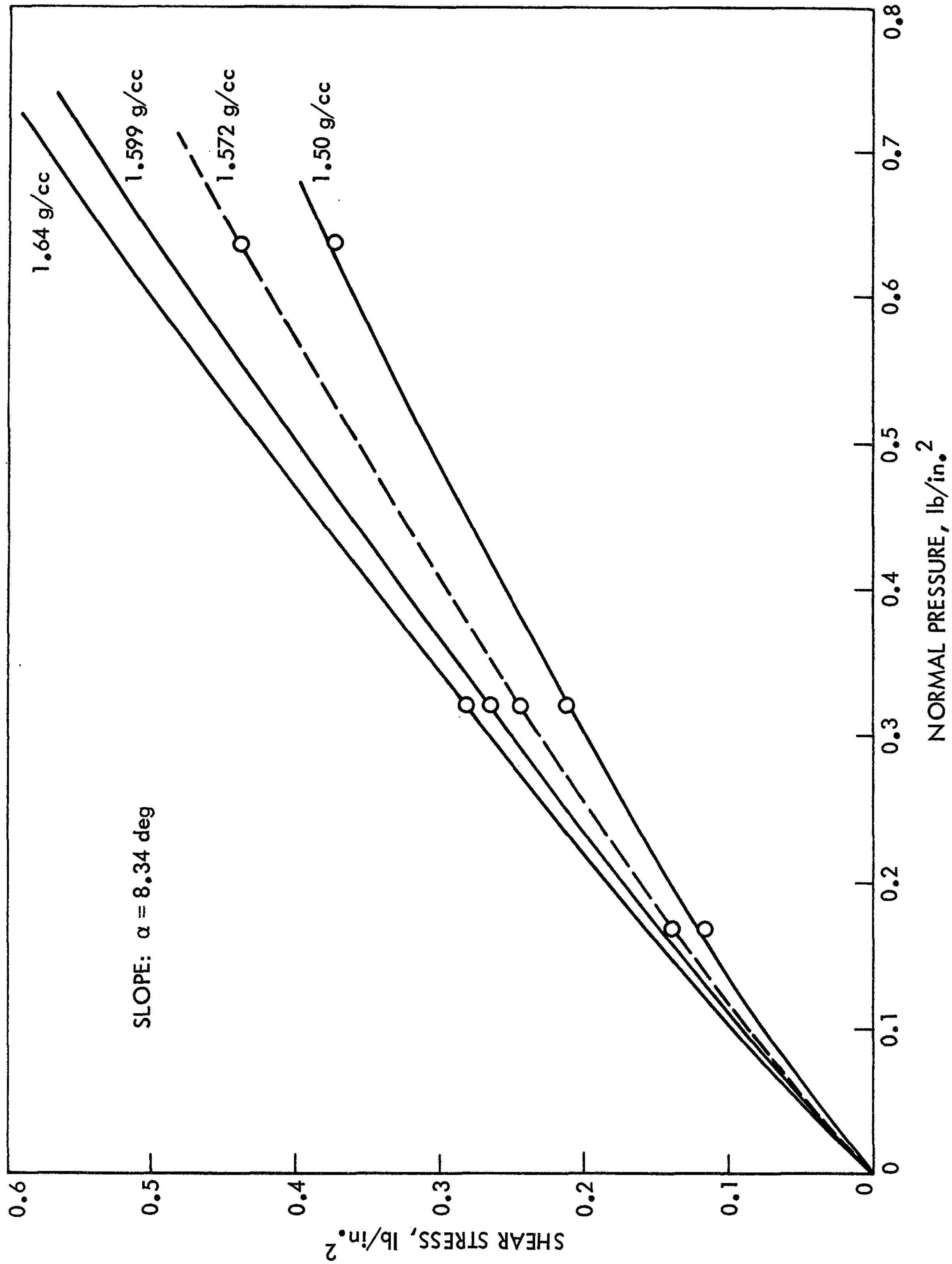

Fig. 23. Sandy Shearing Plate on Soil - Sloped Surface

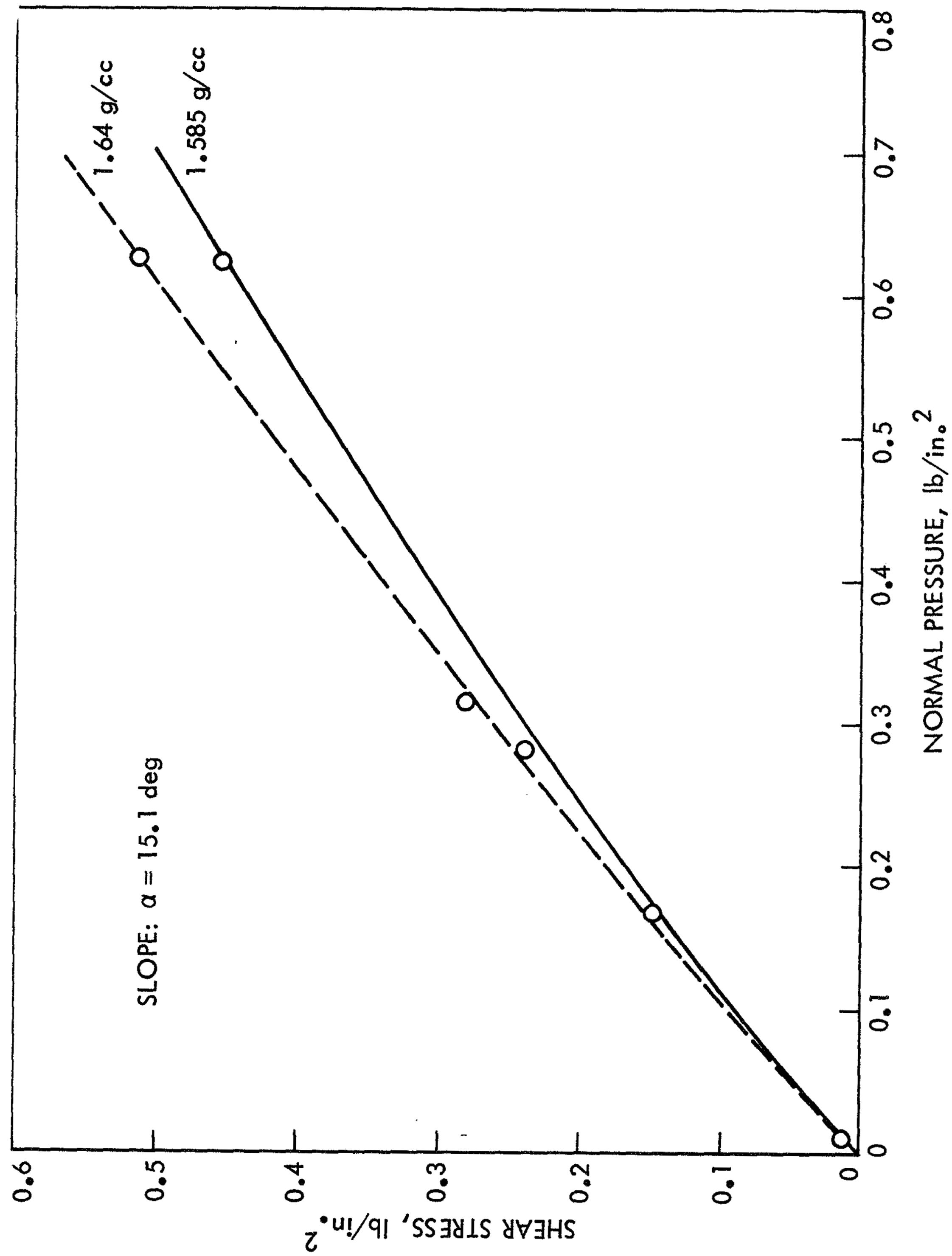

Fig. 24. Sandy Shearing Plate on Soil - Sloped Surface

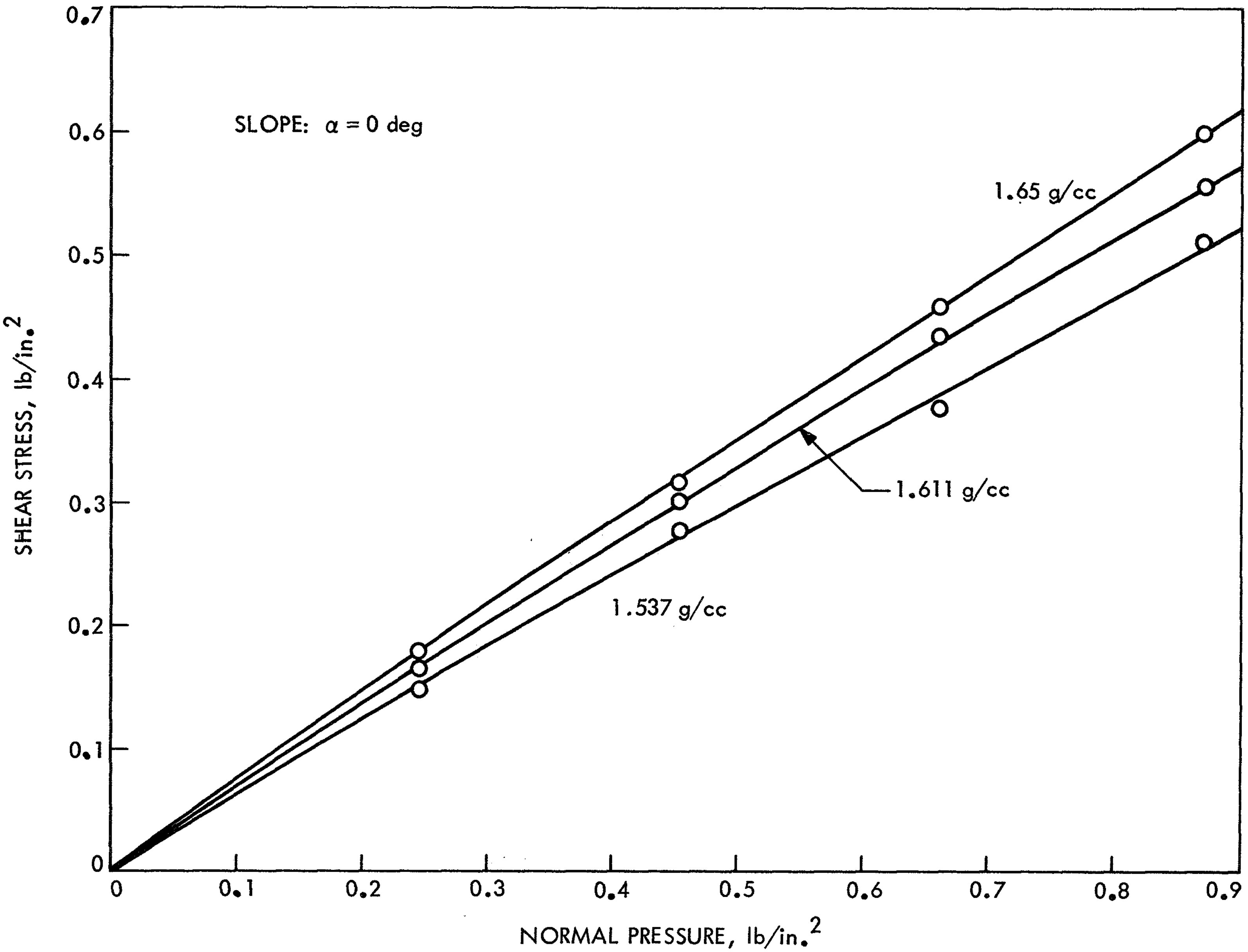

Fig. 25. Shear Test - Rubber Plate on Soil; Level Surface

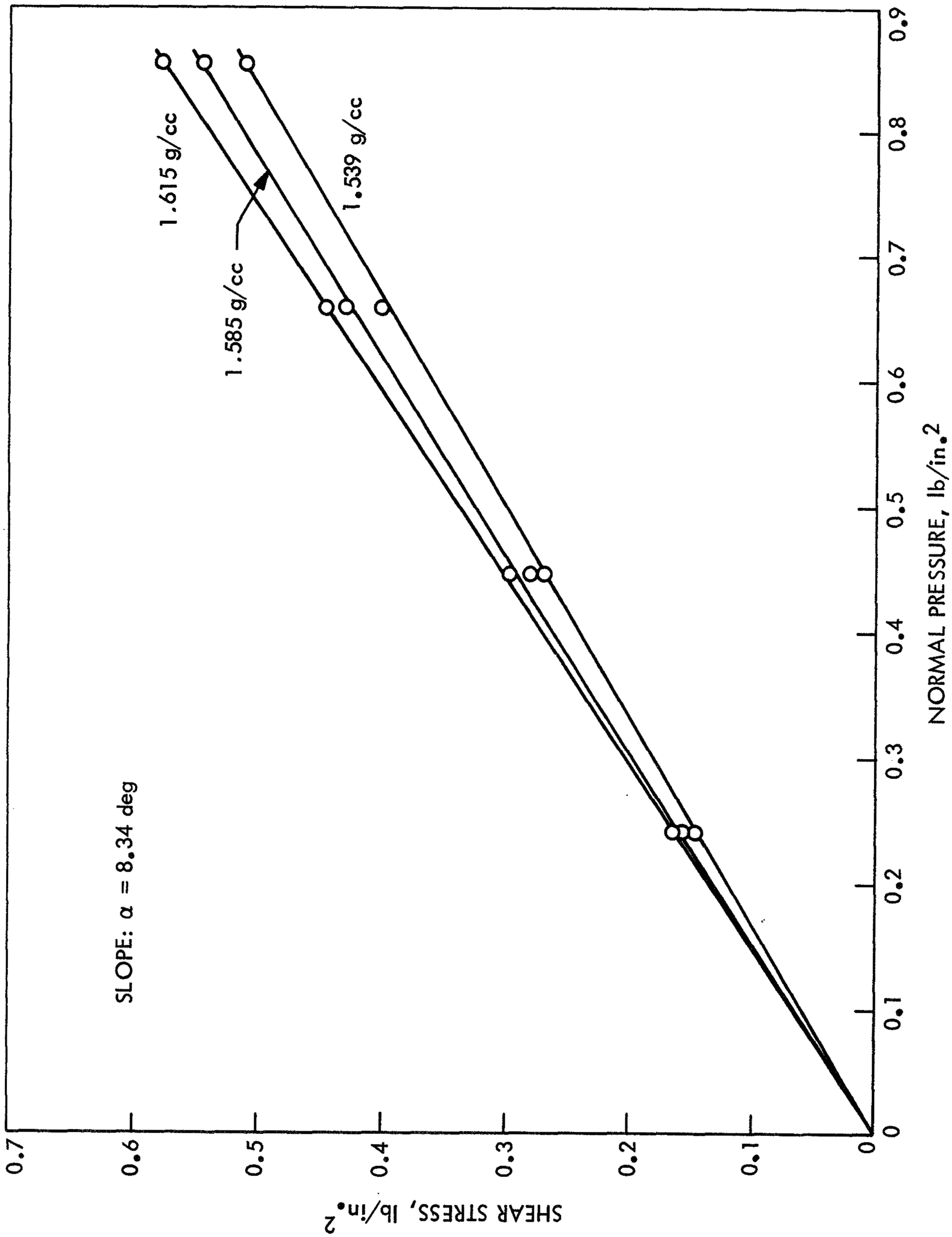

Fig. 26. Shear Test - Rubber Plate on Soil; Sloped Surface

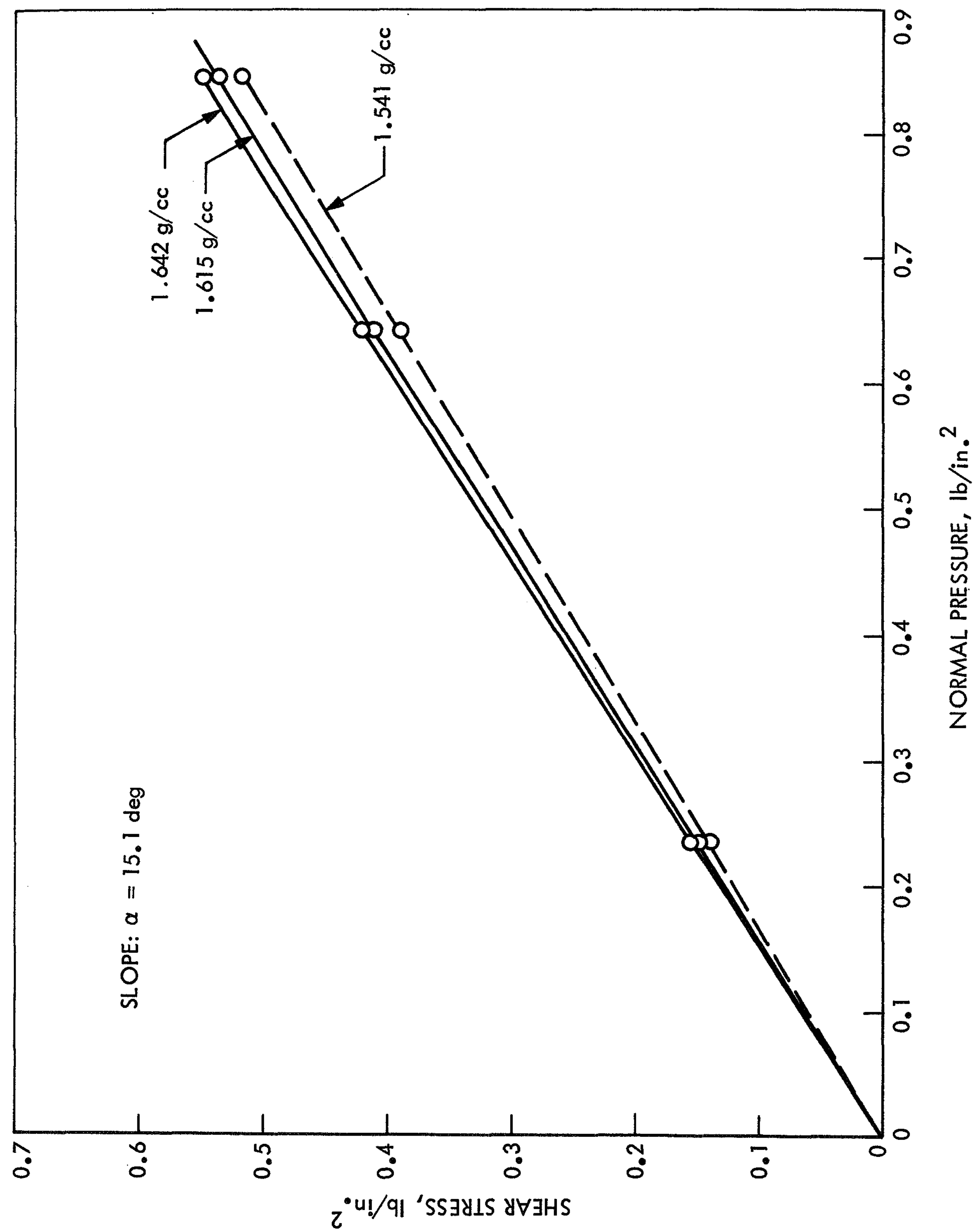

Fig. 27. Shear Test - Rubber Plate on Soil; Sloped Surface

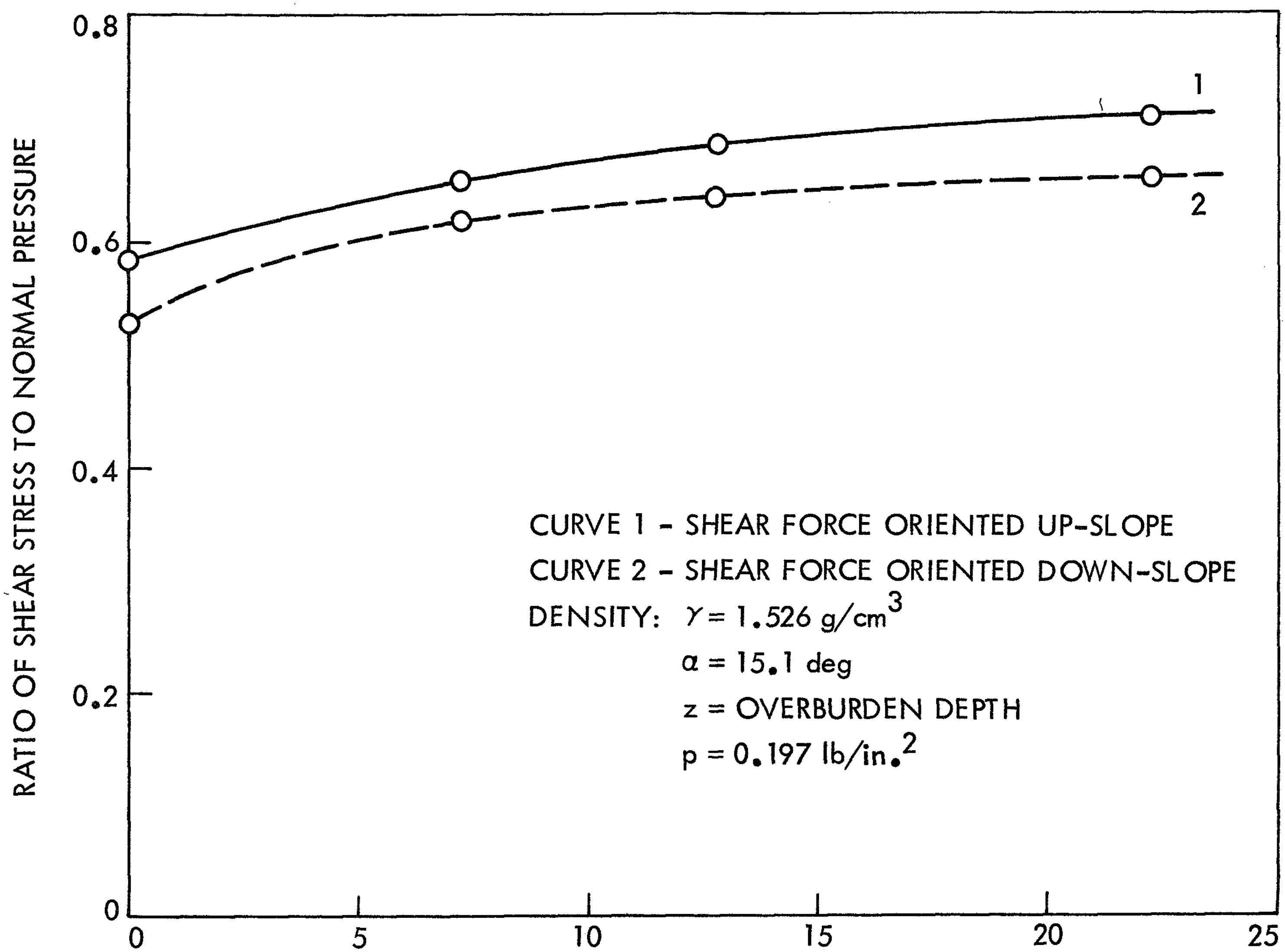

$$C = \frac{\gamma z \cos \alpha}{\gamma z \cos \alpha + p} \times 100\%$$

Fig. 28. Shear Test - Rubber Plate on Silica Sand; Sloped Surface

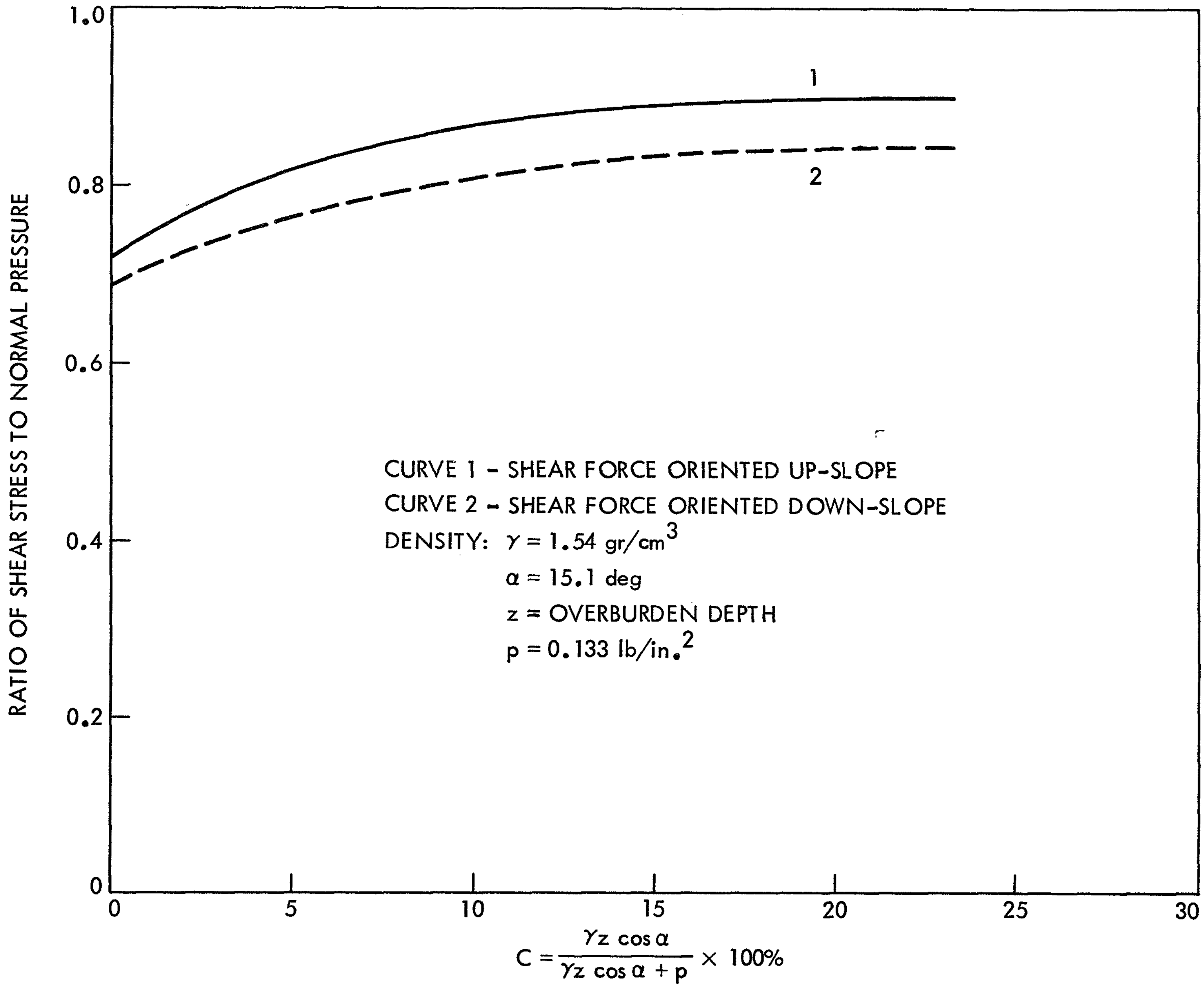

Fig. 29. Shear Test - Sanded Plate on Silica Sand; Sloped Surface

(4) When the shear force is oriented up and parallel to the slope, the soil shearing resistance is higher than when the applied shear force is oriented down and parallel to the slope, Figs. 28 and 29. This condition is viewed as a typical soil slope shearing capacity performance and is dependent on the gravitational field. This behavior does not represent an inherent soil strength property since it does not remain invariant in the directional space. This slope shear strength directional difference is due to the combination of imposed plate, kinematic-stress boundary conditions and soil body forces. This shear directional strength behavior, observed with plate tests, also applies to a wheel when moving up or down a slope. There is an apparent increase of soil-slope stability for a vehicle moving down the slope as opposed to slope climbing. This is due to the orientation of the soil-wheel interface shear forces. In particular, a downhill motion relates to an up-the-slope shear stress orientation. The reverse is true for uphill motion. It may be seen that these factors are also borne out by shear plate test results on sloped surfaces.

(5) For the same relative density, the soil plate interface shear strength increases with the increase of soil confinement ratio, Figs. 28 and 29. This shear strength increase tapers off to a limiting value at a confinement ratio of approximately C = 20.[2]

Any representative surface slope shear tests for mobility purposes should consider the influence of two basic factors: (1) the lateral soil confinement in the potential increase of mobilizable interface friction, and (2) the orientation of the shear stress on the slope surface as affecting its mechanical response.

---

[2] Soil confinement was obtained by adding soil material along the two plate sides, parallel to the shear force. This does not constitute a plate sinkage process, but indicates the controlling influence of lateral soil confinement when sinkage takes place.

IX. ANALYSIS OF TEST RESULTS

A motor driven lunar roving vehicle moving over horizontal and sloping terrains will operate under self-propulsion conditions. Self-propulsion is concerned exclusively with the transport of the vehicle weight. On horizontal terrains, self-propulsion thrust involves the development of a soil-wheel thrust capable of overcoming the rolling resistance of the traction device. On sloping terrain, self-propulsion thrust must equal the combined action of both the rolling resistance and the component of vehicle weight parallel to the slope.

The self-propulsion thrust, T_R, is delivered across the soil-wheel interface, and it is balanced at the wheel axle within the soil-wheel system itself. The T_R vector cannot be measured experimentally as is normally done with the effective draw-bar pull force using a load cell. Measurement of T_R would entail special wheel design and instrumentation requirements; nevertheless, the upper bound of rolling resistance thrust for self-propulsion can be inferred from torque measurements when a steady state condition is reached. Figures 30(a) and 30(b) indicate limiting cases of rolling resistance values, in which the same self-propelling torque, M, is assumed balanced either by the couple

$$M = Wa, \text{ if } T_R = 0, \qquad \text{(no friction)} \qquad \text{Fig. 30(a)}$$

or by

$$M = (\max T_R)\, b, \qquad \text{(maximum friction)} \qquad \text{Fig. 30(b).}$$

Obviously, for a given soil-wheel system the torque, M, has a unique value, but the resultant force, R, and its point of application are not known. Since soil-thrust is due to the frictional nature of the soil-wheel interaction, it is unlikely that either one of the limiting cases shown would prevail. Consequently, T_R should satisfy an intermediate condition,

$$0 < T_R < \max T_R, \text{ as shown in Fig. 30(c).}$$

The resultant reaction, R, must be such that T = Rb, Fig. 30(c).[3]

The direction of the thrust force, T, and the normal force, N, are parallel and normal, respectively, to the original undisturbed surface.

The total soil thrust, T, should account for the combined action of (a) the thrust T_R required to overcome the wheel motion resistance, (b) the weight components parallel to the original terrain slope, and (c) the draw-bar pull force as follows:

$$\frac{T}{N} = \frac{T_R + W \sin\alpha + D.P.}{W \cos\alpha} \; ;$$

where

T = Total soil thrust

T_R = Soil thrust due to rolling resistance

W = Vehicle weight

D. P. = Drawbar pull force

α = Slope angle

The vehicle weight components and draw-bar pull force can be directly measured. For a flexible wheel, the soil thrust force, T_R, arising from the tire rolling resistance is indeterminate,[4] also it is not known to what extent T_R is a function of the loading and slope angle. Therefore, it was decided to evaluate

[3]The apparent lack of uniqueness in determining both the position and orientation of the soil-wheel total reaction, R, can be obviated only if the soil-wheel interaction problem is solved satisfying both the stress equilibrium and kinematic compatibility conditions. In this context, the two dimensional problem of a roller moving on a granular soil slope, with cohesive and frictional properties, is currently being investigated within the realm of soil plasticity theory as a mixed stress and velocity boundary value problem. Viewed in this light, the soil thrust and effective pull are intimately connected and cannot be derived independently of each other.

[4]Though a rolling resistance torque can be measured by tests.

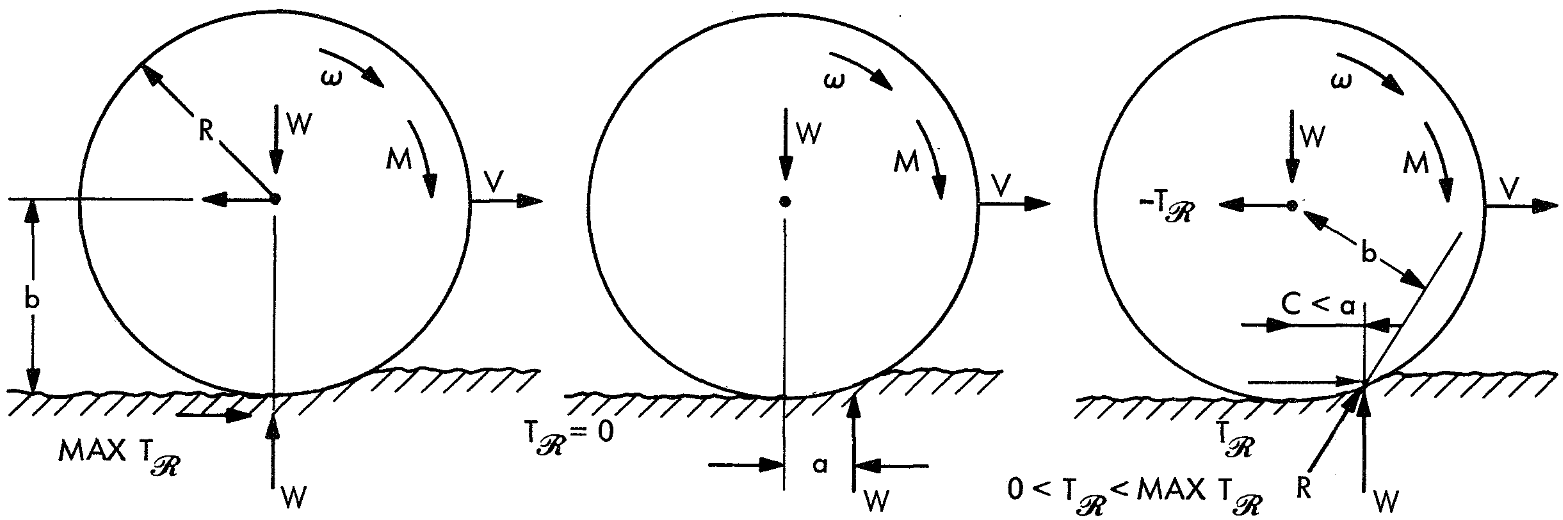

(a) MAX FRICTION (b) NO FRICTION (c) INTERMEDIATE (REAL CASE)

LIMITING CONDITIONS:

M = TORQUE

ω = WHEEL ANGULAR VELOCITY

W = WEIGHT

$T_{\mathscr{R}}$ = SELF PROPULSION THRUST FORCE, ROLLING RESISTANCE

$R = \vec{T}_{\mathscr{R}} + \vec{W}$, TOTAL REACTION

$V = \omega R_{\ell}$ (R_{ℓ} = EFFECTIVE RADIUS)

Fig. 30. Soil - Wheel Thrust Values

vehicle mobility performance in terms of the thrust to normal load ratio (T/N) versus percentage slip, as follows:

$$\frac{T}{N} = \frac{W \sin\alpha + D.P.}{W \cos\alpha} ,$$

$$\text{slip } \% = \frac{V_w - V_v}{V_w} ;$$

where

V_v = Vehicle translational velocity

V_w = Wheel peripheral velocity (in. /sec)

Re = Equivalent wheel turning radius, Table 2, Column (c)

W = Angular velocity, (rad/sec)

The parametric nature of T/N versus slip is evident from Fig. 31. This figure shows that, for each slope and vehicle weight (1W and 1/4W), self-propulsion thrust starts with T/N = tan α at a definite averaged slip value. Increase of D. P. is accompanied by an increase of wheel slip to a limit value of T/N in which the vehicle advances at an extremely slow velocity (slip > 95 percent).

A summary of the performance of vehicle mobility on dry level soil and on dry and wet sloping terrain is given in Table 3.

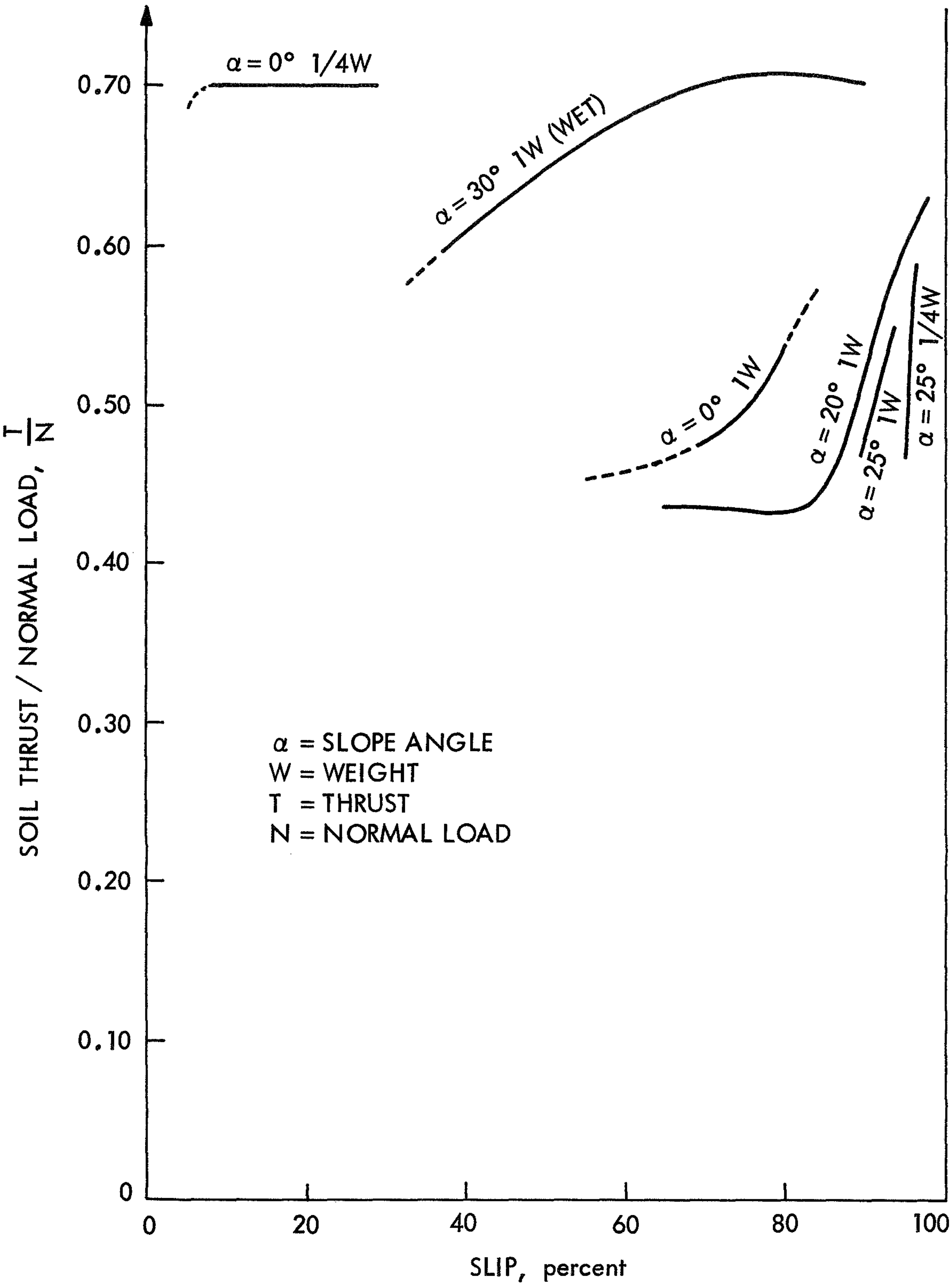

Fig. 31. SLRV Slope Climbing Performance - Thrust/Normal Load Ratio Versus Slip Percentage

Table 3. SLRV Test Results

SLOPE, deg	VEHICLE WEIGHT, lb	NOMINAL TIRE INFLATION PRESSURE, lb/in.^{2}	WHEEL SLIP [a], %	SOIL THRUST TO NORMAL LOAD RATIO [b]	MAXIMUM PULL FORCE, lb	MAXIMUM WHEEL AXLE TORQUES, in./lb		
						FRONT	MIDDLE	REAR
25	158	0.5	90-95	0.465-0.548	12.0	82	43	188
	158	0.25	83-94	0.465-0.52	8.5	98	53	192
	40	0.25	95-96	0.455-0.565	4.0	— [c]	— [c]	— [c]
20	158	0.5	60-97	0.412-0.62	38	101	70	205
0	158	0.5	— [c]-80	0-0.511	81	141	90	241
	40	0.25	14-— [c]	0-0.70	28	34	24	58
30 [d]	158	0.25	32-94	0.576-0.715	19	86	74	229

[a] SLIP PERCENTAGE $S = (V_\omega - V)\,100/V_\omega$, WHERE V_ω = WHEEL PERIPHERAL VELOCITY AND V = WHEEL AXLE TRANSLATIONAL VELOCITY.

[b] SOIL THRUST = LOAD CELL PULL FORCE + VEHICLE WEIGHT COMPONENT PARALLEL TO SLOPE.

[c] DATA REDUCTION NOT AVAILABLE, DUE TO LACK OF RANGE.

[d] WET SAND.

X. CONCLUSIONS

The following are the most important vehicle mobility facts considering low soil-wheel contact pressures:

(1) For horizontal and sloping terrains, far removed from the soil's natural angle of repose, the lower the soil-wheel contact pressure the more significant the improvement of the thrust performance, Fig. 31. This occurs at comparatively reduced slip values and is accompanied by proportionally reduced wheel torques (see 1/4W tests).

(2) The beneficial effect of low contact pressure degrades continuously with increase in the slope. When the slope approaches its natural angle of repose, there is no significant mobility performance gain, either in torque or thrust, regardless of the level of the soil-wheel contact pressure.

(3) Each soil slope, α, is connected with a unique draw-bar pull versus slip performance curve (Fig. 31). This indicates that horizontal wheel tests, as currently done, are inadequate for predicting slope climbing capabilities.

(4) Driven flexible wheels on soft steep slopes (>20 deg) may practically operate at slip values on the order of 50 percent or higher, see Fig. 31. Therefore, current wheel performance evaluation concepts, using fixed slip values of 20-25 percent on horizontal terrains, cannot be applied or extended to evaluate slope climbing performance.

(5) For the same normal load and soil characteristics, the higher the slope the larger the slip percentage required to develop the same thrust force.

(6) On a stable, cohesive, steep soil slope, the overall mobility performance is improved as compared with a cohesionless soil. Viewed as a soil bearing capacity problem, the slope may be

capable of supporting the vehicle load but may be unable to provide the soil-wheel interface thrust friction required to develop vehicle motion. For this test, the SLRV could climb and develop additional pull on a 30 deg wet slope and became immobalized on a 35 deg wet slope. This fact indicates that the soil-wheel interface friction lies between $\mu = 0.63$ to $\mu = 0.68$.

NASA — JPL — Coml., L.A., Calif.